AD NUMBER: AD0335627
CLASSIFICATION CHANGES
TO: Unclassified
FROM: Confidential
LIMITATION CHANGES
TO: Approved for public release; distribution is unlimited.
FROM: Distribution authorized to U.S. Gov't. agencies and their contractors; Administrative/Operational Use; 31 DEC 1960. Other requests shall be referred to Office of Naval Research, Arlington, VA 22203.
AUTHORITY
c to u and c/2 to a/1 per doc markings

GENERAL DECLASSIFICATION SCHEDULE

IN ACCORDANCE WITH
DOD 5200.1-R & EXECUTIVE ORDER 11652

THIS DOCUMENT IS:

CLASSIFIED BY_____

Subject to General Declassification Schedule of Executive Order 11652-Automatically Downgraded at 2 Years Intervals- DECLASSIFIED ON DECEMBER 31, 7[illegible].

BY

Defense Documentation Center
Defense Supply Agency
Cameron Station
Alexandria, Virginia 22314

CONFIDENTIAL

MC-61-6-R1

RAIN EROSION SUPPRESSION AT SUPERSONIC SPEEDS (U)

BURTON D. FIGLER
WILLIAM J. PARKIN
JOE C. WILSON, JR.

OCTOBER 1962

Group 4

MITHRAS, INC.
MICROWAVE AND THERMAL RADIATION SENSORS
380 PUTNAM AVENUE, CAMBRIDGE 39, MASS.

CONFIDENTIAL

CONFIDENTIAL

MITHRAS, INC.
380 Putnam Avenue
Cambridge 39, Massachusetts

MC-61-6-R1

RAIN EROSION SUPPRESSION AT SUPERSONIC SPEEDS (U)

by

Burton D. Figler
William J. Parkin
Joe C. Wilson, Jr.

Interim Engineering Report
Nonr Contract 3684(00)

October 1962

98 p. incl. illus table

This report contains
xii and 98 pages.

Copy No. 79

MS Log 923

CONFIDENTIAL

FOREWORD

The research reported herein is directed toward the reduction of rain erosion in high speed vehicles. It is being sponsored by the Department of the Navy's Office of Naval Research and Bureau of Naval Weapons under Contract Nonr 3684(00). Scientific Officer for ONR Air Programs is Lt. Cmdr. Stuart D. Kearney; and for BuWeps Missile Division, Mr. James M. Lee.

This is an interim report covering the first year's activity under a planned two-year program.

MITHRAS, for itself, and on behalf of its sponsor, the Navy, expresses its appreciation to Professor Edward S. Taylor of the Massachusetts Institute of Technology for generously making available the facilities and excellent support of the Gas Turbine Laboratory. Use of these facilities resulted in substantial savings of time and money and helped to hasten the day when the product of this research can be applied to our country's weapons.

TABLE OF CONTENTS

TABLE OF CONTENTS (Continued)

LIST OF FIGURES

LIST OF FIGURES (Continued)

LIST OF FIGURES (Concluded)

LIST OF TABLES

LIST OF SYMBOLS

A	area
a	speed of sound; constant
C	speed of sound; constant
C_f	friction coefficient
D	diameter; distance
d	pit diameter
f	force
h	height
K	constant
L	constant
ℓ	length
M	Mach number
m	mass
$\dot{m}$	mass flow
p	penetration; pressure
q	dynamic pressure
R	Rankine; gas constant
r	radius
Re	Reynold's number
T	temperature
t	time
u	velocity
V	volume, velocity
v	jet velocity

LIST OF SYMBOLS (Continued)

x	distance; final drop diameter; compressibility
α	constant
β	constant
δ	deviation from spherical shape
μ	absolute viscosity
ν	kinematic viscosity
ρ	density
σ	surface tension
ϕ	angle

Subscripts

a	air
b	breakup
crit	conditions at which drop breakup begins
cyl	cylinder
H_2O	water
i	initial; internal
j	jet
ℓ	length
s	shoulder of drop
st	surface tension
t	target; stagnation conditions
w	water; wetted
0	accumulator
1	conditions upstream of a normal shock

LIST OF SYMBOLS (Concluded)

2	conditions downstream of a normal shock
∞	conditions at infinity

Superscripts

*	conditions at a sonic throat

1. SUMMARY

Both theoretical and experimental data indicate that a properly designed flow-separating spike, mounted in front of a radome, will produce a "dead air" region of sufficient depth to cause breakup of oncoming raindrops and thereby significantly reduce the erosion damage to the radome. Equations, based on the experimentally observed breakup process of water drops, have been developed to predict the drop breakup distance and drop breakup time.

An erosion simulation system has been designed and the water injection and photographic sub-systems have been used in a number of tests conducted in a Mach 2 airstream. These tests have indicated the utility of flow separation devices in shattering raindrops and show that protection, ranging from fair to excellent, will be afforded the radome by the use of such devices.

2. INTRODUCTION

Raindrop impingement on radomes of operational missiles and aircraft traveling at speeds in excess of M = 0.75 causes rapid pitting and eroding of the domes, thus seriously restricting the operational use of these vehicles in bad weather. Moreover, when erosion does occur, it affects not only the structural integrity of the dome but also its radar transmission characteristics. All known materials show rain erosion damage if exposed for a sufficiently long period of time at Mach numbers in excess of 0.75, and this is especially true of the glass reinforced plastic laminates currently used in aircraft and missile radomes. These cannot withstand more than a few minutes of one-inch-per-hour rainfall at 500 mph and drastically less at higher velocities.

Although a substantial amount of experimental data has been collected on rain erosion at subsonic velocities, data on supersonic erosion phenomena is virtually non-existent, primarily because of a dearth of suitable facilities. Sled tests have been used in an attempt to study erosion at supersonic speeds but these tests are unreliable and far too expensive. Problems of vibration and sled design are extremely severe, and data collection is difficult at best. In recent years several limited studies have been made of the raindrop breakup process in high speed flows but these have been complicated by an inability to create actual raindrops in supersonic flows. Without developing a general understanding of the phenomenon, it was determined that under certain conditions of relative velocity between air and drop, the drop would break up into smaller particles. It was also known that the amount of damage resulting from particle impingement is closely related to the size of the particle.

At this stage MITHRAS proposed to the Navy a solution to the erosion problem based on the use of a spike projecting from the nose of a missile. A properly designed nose spike will produce a "dead air" region immediately in front of a missile. The relative velocity of this dead air region, it was

proposed, differed enough from that of the oncoming air and raindrop so as to induce breakup of the raindrop before it could strike the radome.

In response to its proposal, MITHRAS was awarded, in late 1961, Contract Nonr 3684(00) to undertake the following:

1. An experimental and analytical determination of the behavior of water drops in supersonic air streams;
2. An experimental and analytical determination of the effects of water drop impact on radome materials; and,
3. The testing and evaluation of the effectiveness of a flow separating spike as a means of protecting a radome against raindrop damage or destruction.

This was visualized as a two-year program. This report describes the research accomplished during the first year, which has more than achieved its intended goal. Recommendations for carrying the research forward further and faster than originally contemplated will be made.

At the start of the program it was obvious that an essential requirement was a simple, economical, and versatile laboratory facility in which to create and break up raindrops. For this purpose, MITHRAS, Inc., undertook the design and construction of a rain erosion simulator.

The simulator has two basic components: a raindrop injection system which will produce water drops of controllable size at the desired frequency, and an air flow system which can produce supersonic air flows of the desired Mach number, density, temperature, etc. In combination these produce a special small wind tunnel in which desired conditions of rain can be established for the three basic tasks:

1. The study of raindrop breakup
2. The measurement and observation of the actual effects of raindrop impact on any radome material
3. The development of protective devices to minimize the damage caused by raindrop impact

The design of the simulator for the study of the rain erosion process, material testing, drop breakup phenomenon, and erosion alleviating devices, has been completed. Much of the equipment, including the photographic and water injection systems, has been constructed and successfully operated.

A number of tests have been conducted in a supersonic airstream, at Mach 2, employing the water injection and photographic systems, to determine the feasibility of utilizing flow separation techniques for shattering raindrops. These tests show that raindrops can be shattered by this technique and that protection, ranging from fair to excellent, will be afforded the radome.

During the next year it will be necessary to complete and refine the test apparatus. The speed of the photographic system will be improved substantially; and a decision will be reached as to the desirability of continuing to use a closed return air stream or whether to convert to an open return. Tests and analyses will then proceed as rapidly as possible on all three tasks.

It is anticipated that the research during this second year will provide a firm basis for the intelligent design of spiked radomes that will be relatively safe from the effects of high speed flight through rain.

3. REVIEW OF WORK ON THE RAIN EROSION PROBLEM

With the advent of operational supersonic aircraft and missiles, the problem of rain erosion has assumed far greater significance. As the importance of this problem began to be recognized, some rudimentary attempts were made to study the nature and severity of damage produced on typical radome materials. These studies employed, among other methods, sled tests through simulated rain fields; actual flight tests through rainstorms; whirling arm devices that traversed simulated rain fields; the firing of solid pellets (which were supposed to simulate water drops) into test materials; and the firing of solid pellets into raindrops.

Many of the reports referenced in the following pages contain information on the search for erosion resistant radome materials and protective coatings for radomes. At best, this research has only been partially successful and the need for erosion resistant materials and for methods of minimizing erosion damage is still of the utmost urgency.

Research on both materials and methods up to now has been further complicated by a very incomplete understanding of drop behavior in high speed air streams, and in fact by an inability to generate discrete, controllable, drops in a supersonic stream.

3.1 Testing Methods for Determining Erosion Damage

Descriptions of the various test methods and the results obtained, as well as the various damage mechanism theories expounded, are included in References 1 through 19. The usefulness of most of these testing schemes and the data thereby acquired is open to considerable doubt. For example, the whirling arm device cannot attain velocities above approximately 550 mph; the firing of solid pellets into sample target materials has never been shown to be equivalent to liquid drop impacts on radomes; and actual flight tests of aircraft in rain are extremely unpopular with the pilots performing such tests because of the substantial risk involved. As a result, flight tests have never been seriously attempted on a large scale.

Despite their limitations, these various tests all confirmed the fact that radomes were highly susceptible to rain erosion damage and that some manner of protection was urgently needed. Various new materials have been developed and protective coatings, e.g., neoprene, have been applied to typical radomes. In some cases, minor improvement was obtained but no real cure to the problem has been developed by this approach.

The damage equations formulated for target pitting by earlier investigators are in some agreement and can be summarized as

$$\frac{p}{d} = K \left(\frac{\rho_p}{\rho_T}\right)^{\alpha} \left(\frac{V}{C}\right)^{\beta} \qquad (3.1)$$

where

p = penetration of projectile (solid or liquid) into the target

d = diameter of projectile

K, α, β = constants dependent upon target material and projectile

V = projectile velocity

C = speed of sound in target material

For solid projectiles fired into solid targets, there is some evidence that α and β may be on the order of 2/3. Theoretical considerations can also lead to this value for α and β.

Unfortunately other types of target damage such as spalling, cracking, and delamination, were not considered in detail and, to this author's knowledge, no equations have been developed to predict damage of this sort.

3.2 Water Drop Breakup in Subsonic and Supersonic Airstreams

Several authors have studied the behavior of water drops in regions of high velocity air. These studies are included in References 20 to 30. They describe a number of ingenious methods for obtaining photographs of the drops while they are immersed in regions of high subsonic airflow. Unfortunately, no one has been able to obtain photographs of good enough quality to show clearly the drop breakup process in supersonic airstreams.

Some effort has been made to describe, with reasonably simple theories, the breakup process and for the subsonic case, these theories have been substantiated, in a gross sense, by the experimental data available. For the supersonic case, the experimental data is so limited that no substantiation is feasible.

3.3 Supersonic Water Jets

For a careful and systematic study of the drop breakup process, and of the effects of erosion, it was necessary to be able to create drops of the desired size and velocity in a supersonic stream of air.

In order to obtain drops of the desired size and velocity, it was determined that the water must be injected into the supersonic airstream in the form of a thin jet, and at a velocity comparable to that of the airstream. This jet quickly breaks up into discrete drops of controllable size and velocity.

A literature search disclosed almost no work in the area of high velocity jet behavior in supersonic airstreams. The work that had been done (References 31 to 35) was primarily concerned with atomization of injected fuels and oxidizers into combustion chambers.

What information was available indicated that the process of the jet breakup into the desired drops was largely controlled by the relative velocity between the jet and the airstream with relatively minor effects produced by jet orifice geometry, ambient pressure, and absolute jet velocity. The size of the drops produced from the jet could be related to this relative velocity and in turn to the pressure required to eject the water at the desired velocity.

4. MITHRAS' SOLUTION TO THE RAIN EROSION PROBLEM

While a general understanding of the physical process of drop breakup has not been achieved, several pertinent facts have been uncovered by investigators.

It has been found that, for a given drop size, there is a critical relative velocity between the air and the drop above which drop breakup occurs and below which no breakup occurs. Figure 1, replotted from Ref. 29, plots the critical velocity against drop size. It is readily apparent from Fig. 1 that for the velocities which we are considering, i.e., supersonic velocities, drop breakup can always be expected to occur. The actual breakup process is apparently dependent upon the difference in velocity between the drop and the air and does not appear to be directly affected by the shock preceding the vehicle.

Experimentally it has been determined that at least three different breakup processes exist: (1), a vibrational mode whereby the drop vibrates with an increasing amplitude until the drop shatters, (2), a process in which the drop first inflates like a parachute and then bursts in the center, and, (3), a stripping action whereby liquid is stripped off the periphery of the drop. The first type of breakup is a rather slow process and apparently does not have time to develop if the relative velocity is very high, as in the case of a supersonic relative velocity.

The blowing-out type of process has been experimentally observed and has been considered by Gordon in Ref. 21. Gordon finds that for a liquid of low viscosity, e.g., water, the time for drop breakup, assuming the second type of breakup, is given by

$$t_b = \frac{2 D_i}{V} \left(\frac{\rho_w}{\rho_a}\right)^{1/2} \qquad (4.1)$$

where

t_b = "breakup time"

D_i = initial drop diameter

V = relative velocity between drop and airstream

ρ_w = density of drop

ρ_a = density of air

Hinze, in Ref. 23, using other arguments than Gordon, arrived at the following relation

$$t_b = \frac{2D_i}{V} \left(\frac{\rho_w}{\rho_a}\right)^{1/2} \left[\frac{1}{2} \sqrt{\frac{2}{3}} \left(\frac{\delta}{D}\right)_{crit} \right] \qquad (4.2)$$

where

δ = deviation from the spherical shape at the stagnation point

the subscript indicates the value at which drop breakup first occurs

Hinze finds experimentally that

$$\left(\frac{\delta}{D}\right)_{crit} \approx 0.655$$

so that

$$t_b \cong (0.33) \frac{2D_i}{V} \left(\frac{\rho_w}{\rho_a}\right)^{1/2} \qquad (4.2a)$$

It can be seen that Eqs. (4.1) and (4.2a) are almost identical. Either equation may be given a physical, though artificial, interpretation if the two expressions for the "breakup time" are rewritten as

$$t_b \approx \sqrt{\frac{\left[\frac{\pi D_i^2}{4} \rho_w \ell\right] / \ell}{\frac{1}{2} \rho_A V^2}} \qquad (4.3)$$

If we now consider the drop to be a cylinder of water of diameter D_i and length ℓ with pressure $p_a = \frac{1}{2} \rho_a V^2$ acting on the cylinder face (see Fig. 2), then the square of the breakup time becomes proportional to the mass per unit length of the fictitious cylinder and inversely proportional to the pressure acting on the cylinder face. The question of what constant of proportionality is to be used in Eq. (4.3), or which of the two equations, (4.1) and (4.2a), should be used, is relatively unimportant since either relation will give results that are of the same order of magnitude. Also, the question of what precisely is meant by "breakup time" has not been answered. Equation (4.1) was used to compute "breakup times" for comparison with the shock tube data obtained by Engel (Ref. 20). The following table illustrates the results obtained.

Shock Mach Number	Relative air velocity behind the shock	t_b (experimental)	t_b (Eq. 4.1)
1.3	498 ft/sec	greater than 743 μ sec	1000 μ sec
1.5	777 ft/sec	less than 764 μ sec	663 μ sec
1.7	1035 ft/sec	less than 594 μ sec	497 μ sec

In all cases the calculated values give results that are consistent with the experimental data. It should be borne in mind that the experimental values of t_b could not be estimated to better than 30 or 40 percent so that the calculated values are in good agreement with the experimentally determined values.

One fact, and a very important one, that as yet has not been mentioned, is that the data of Ref. 20 appears to be that resulting from the third type of breakup, yet Eq. (4.1), which was derived for the second type of breakup, still gives reasonable results. It has been pointed out by several authors that the stripping type of breakup is the one to be expected at supersonic speeds (Refs. 21, 26, 30). It would, therefore, appear that Eq. (4.1) provides a reasonable first estimate of the "breakup time" of water drops in a supersonic airstream. Although the equation has been developed for the

blowing out type of drop breakup, it appears to be also applicable for the stripping type of breakup.

Equation (4.1) has been found to agree reasonably well with experimental data as has been indicated. It was a matter of concern, however, that the breakup model which led to Eq. (4.1) did not agree with the experimentally observed breakup phenomenon at high (supersonic) speed.

It should be remembered that Eq. (4.1) was derived on the basis of the following breakup process:

1. The high pressure at the stagnation point of the drop blows the drop inward like a balloon (see Fig. 3).
2. The center of the "balloon" blows out and the drop shatters (see Fig. 4).

This type of drop breakup does indeed occur at moderate speeds (a few hundred feet per second) but not at supersonic velocities. The question then naturally arose as to why Eq. (4.1) provided good results at supersonic velocities.

It was experimentally observed that at supersonic velocities the drop breakup process is made up of a stripping action as indicated in Fig. 5. This stripping action can be represented by the tearing off of an annulus of water at the shoulder of the drop.

At the shoulder of the drop, where the stripping occurs, the pressure loading is approximately zero since the air flow nearly has returned to its original direction. Indeed, the familiar cosine square pressure distribution which is often used to approximate the pressure loading over hemispheres does go to zero at the shoulder. The friction force arising from viscous effects, however, is a maximum at the shoulder. We will, therefore, assume that the friction forces and surface tension forces are the only forces acting in the vicinity of the shoulder. We can represent this situation by the sketch appearing on the following page.

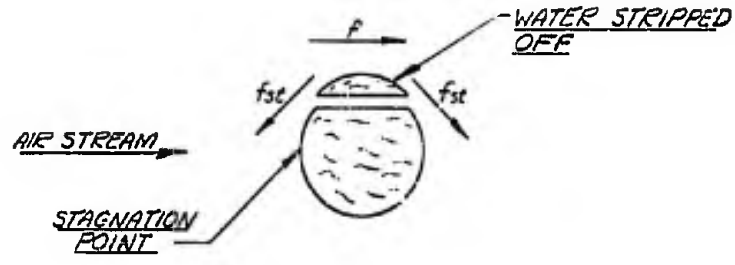

f = friction force in pounds

f_{st} = surface tension force in pounds

It must be noted that the sketch above is a cross section of the drop and in reality the stripping process takes place over an annulus whose axis is lined up with the air stream. We will assume that the stripping takes place over a small region around the shoulder. This assumption will be looked at more closely at a later stage in the derivation of the breakup time.

With the assumption that stripping occurs within a small region around the shoulder, we can use the following approximations:

1. f_{st} and f have nearly the same line of action, i.e., they are parallel (or anti-parallel).
2. The water stripped off can be approximated by a hollow cylinder of thickness a r and length h (see Fig. 6).

The cross sectional area of the hollow water cylinder torn off is given by

$$A = \text{area} = \frac{\phi}{2\pi} \pi (r + a\,r)^2 - \frac{h\,r}{2}$$

$$\phi \cong \frac{h}{r}$$

$$A = \frac{h\,r}{2} (1 + a)^2 - \frac{h\,r}{2}$$

$$(1 + a)^2 \cong 1 + 2a, \text{ for } a^2 << 1 + 2a$$

thus

$$A \cong h\, r\, a$$

thus the thickness of the equivalent hollow cylinder is a r.

Surface area of cylinder = A_w

$$A_w = 2 \pi r h \qquad \text{for } a << 1 \qquad (4.4)$$

Volume of cylinder = V

$$V = 2 \pi r^2 h a \qquad (4.5)$$

Length of annulus over which surface tension acts = ℓ

$$\ell = 2 \pi r \qquad (4.6)$$

and

$$f_{st} = \sigma\, 2 \pi r \qquad (4.7)$$

where

σ = surface tension in pounds per inch.

For water the surface tension is given in Ref. 36 as

$$\sigma = 4.81 \times 10^{-4} \ \frac{lb}{in.} \qquad (4.8)$$

The friction force can be computed as follows:

$$f = \frac{1}{2} \rho\, V^2\, C_f\, A_w \qquad (4.9)$$

V = the relative velocity between the drop and the air in feet per second

C_f = friction coefficient

A_w = wetted area

ρ = air density in slugs per cubic foot

Looking at a cross section of the cylinder of water that is stripped off,

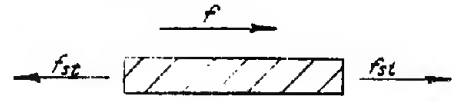

we can define the drop breakup to occur when

$$f = f_{st} \tag{4.10}$$

and this constraint also determines the value of a as follows:

$$f = \frac{1}{2} \rho \ V^2 C_f A_w = f_{st} = \sigma \ell \tag{4.11}$$

but

$$\frac{1}{2} \rho \ V^2 C_f \, 2 \pi \, r \, h = \sigma \, 2 \pi \, r$$

$$(\frac{h}{2})^2 + r^2 = (r + a \, r)^2$$

and

$$h = 2 r \sqrt{a(a + 2)} \cong D \sqrt{2a} \quad \text{for} \quad a << 2 \tag{4.11a}$$

$$A_w \cong \pi \, D^2 \sqrt{2a} \tag{4.12}$$

Combining (4.11) and (4.12), we get

$$\frac{1}{2} \rho \, V^2 C_f \, D \sqrt{2a} = \sigma$$

or

$$\sigma = q \, C_f \, D \sqrt{2a}$$

where

$$q = \frac{1}{2} \rho \, V^2 \quad = \text{dynamic pressure}$$

and

$$a = \frac{1}{2} \ \frac{\sigma^2}{q^2 \, C_f^{\,2} \, D^2} = \frac{1}{2} \ (\frac{\sigma}{q \, C_f \, D})^2 \tag{4.13}$$

We can approximate C_f by the friction coefficient on a flat plate. To do this we compute

$$Re_s = \frac{\rho_s V_s \frac{\pi D}{4}}{\mu_s} \tag{4.14}$$

where

Re = Reynolds number

ρ = density in pounds per cubic foot

V = relative velocity between the drop and the air

D = drop diameter

μ = viscosity in $(\text{pounds})_{\text{mass}}$ per foot-second

The subscript s refers to conditions at the shoulder. Using this value of Reynolds number and Fig. 21.4 of Ref. 37, we can determine C_f for a given drop Mach number and from Eq. (4.13) we can determine a. At this point we have computed f, f_{st}, and a, and knowing D, V, ρ_w, and ρ_a, we can compute t_b as follows.

The drop will be considered as broken up when the stripped cylinder has traveled a drop diameter since it has then completely separated from the original drop. The force equation on the stripped cylinder can be determined by considering the following figure.

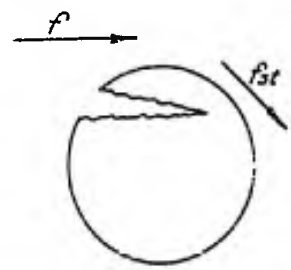

In the condition illustrated, the front portion of the stripped cylinder has separated from the main portion of the drop and we now wish to compute the time for the cylinder to travel one drop diameter.

$$\sum F = f + f_{st} = m \frac{dv}{dt} \tag{4.15}$$

but we have from Eq. (4.10)

$$f = f_{st}$$

so that

$$2f = m \frac{dv}{dt}$$

where

m = mass of stripped cylinder in slugs

v = velocity of stripped cylinder in ft per sec

$$v = \frac{2ft}{m} + C_1$$

at

$$\left.\begin{aligned} t &= 0 \\ v &= 0 \end{aligned}\right\} \; C_1 = 0$$

at

$$x = \frac{2ft^2}{2m} + C_2$$

$$t = 0$$

$$x = 0, \; C_2 = 0$$

and for $x = D$

$$t_b = \sqrt{\frac{m D}{f}} \qquad (4.16)$$

Using Eq. (4.11) and Eq. (4.12)

$$t_b = \sqrt{\frac{2m}{\rho \, v^2 \, C_f \sqrt{2a} \, \pi D}} \qquad (4.17)$$

From Eq. (4.5) we can compute m as

$$m = \rho_w V = \rho_w \frac{\pi D^2}{2} ha$$

and with the help of Eq. (4.11a)

$$m = \rho_w \left[\frac{\pi D^2}{2}\right] \left[D\sqrt{2} \; a^{3/2}\right] \qquad (4.18)$$

Combining Eqs. (4. 17) and (4. 18)

$$t_b = \sqrt{\frac{\rho_w D^2 a}{\rho_a V^2 C_f}} = \left[\sqrt{\frac{a}{C_f}}\right] \frac{D}{V} \sqrt{\frac{\rho_w}{\rho_a}} \qquad (4.19)$$

Equations (4. 19) and (4. 1) are now seen to be identical if $\sqrt{a/C_f}$ is identified with C and if Eq. (4. 1) is written as

$$t_b = C \frac{D_i}{V} \sqrt{\frac{\rho_w}{\rho_a}}$$

The computation of C follows quite easily. Let us consider a drop with

$$D = 0.040"$$

$$V = 1682 \text{ ft/sec}$$

$$\rho_w = 62.4 \text{ lb}_m/\text{ft}^3$$

We will consider the drop in a wind tunnel at Mach number 2, with $p_0 = 30$ psi and $T_{0_t} = 560°$ R. The drop will be assumed to enter a still air region behind a normal shock at a velocity of 1682 ft/sec. Then we have

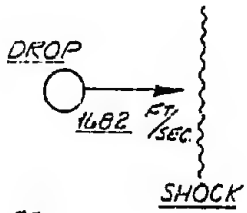

$\rho_{t_2} = .0935$ lb/FT^3 $= \rho_a$

$V_a = 1682$ FT/SEC $\qquad V_a = 0$

$$Re_s = \frac{\rho_s V \pi \frac{D}{4}}{\mu_s}$$

$$= \frac{0.0935 \times 1682 \times \frac{\pi \times 0.04}{4 \times 12}}{130 \times 10^{-7}} = 3.16 \times 10^4$$

(the value of μ_s is obtained from Ref. 38).

From Fig. 21.4 of Ref. 37, we obtain

$$C_f = 7 \times 10^{-3}$$

$$q_s = \frac{1}{2} \rho_s V^2 = \frac{1}{2} \times \frac{0.0935}{32.2} \times (1682)^2 = 4.11 \times 10^3 \frac{lb}{ft^2}$$

Equation (4.13) can now be solved for a as follows:

$$a = \frac{1}{2} \left[\frac{\sigma}{q C_f D} \right]^2$$

$$a = 18.1 \times 10^{-4}$$

The small value of a which is obtained thus justifies the assumption that stripping occurs only over a small area at the shoulder. C is computed as

$$C = \sqrt{\frac{a}{C_f}} = 0.509$$

thus

$$t_b = 0.509 \frac{D}{V} \sqrt{\frac{\rho_w}{\rho_a}} \qquad (4.20)$$

which is in close agreement with the given values of C (0.66 to 2).

In reality, of course, t_b should be some fraction of the total breakup time or it may be considered to be a "breakup time-constant" so that the breakup time is then some multiple of the breakup time-constant. The derivation just concluded cannot provide the value of this multiplying factor and it must be determined experimentally. Whether any practical derivation of the drop breakup time can predict the value of this multiplicative constant is open to serious doubt.

We can obtain the value of C_f for a cylinder and use this value to approximate C_f for the drop.

C_f for a cylinder is given in Fig. 9.7 of Ref. 37 as

$$C_f \sqrt{\frac{V_\infty r}{\nu}} = 2.6 = C_f \sqrt{\frac{V_\infty \rho r}{\mu}}$$

$V_\infty = 1682$ ft/sec

$r = 0.02/12$ ft

$\rho = 0.0935\ lb_m/ft^3$

$\mu = 130 \times 10^{-7}\ \frac{lb_m}{ft\text{-}sec}$

$\nu = \frac{\mu}{\rho} = 13.9 \times 10^{-5}\ \frac{ft^3}{ft\text{-}sec}$

$V_\infty r = 2.80\ \frac{ft^2}{sec}$

$C_f = 2.6 \sqrt{\frac{\nu}{V_\infty r}} = 2.6 \sqrt{4.97 \times 10^{-5}} = 0.0183$

$(C_f)_{cyl.} \cong \sqrt{3}\ (C_f)_{flat\ plate}$

$a = 0\ 00181$

$\frac{a}{C_f} = 0.1$

$\sqrt{a/C_f} = 0.316$ (which again is in good agreement with existing data) (4 21)

The value of C_f which is actually correct is of academic concern since in reality the friction force will change during the breakup process The determination of C_f as a function of time would be nearly impossible and the usefulness of the result of this determination is open to doubt. In any event, the important results of the derivation just carried out are the functional dependence of the breakup time on the drop diameter, water density, relative velocity, and air density.

The value of C can be related to air stream and drop parameters as follows:

$$a = \frac{1}{2}\left[\frac{\sigma}{q\,C_f\,D}\right]^2$$

$$C_f = \frac{2.7}{\sqrt{Re_\ell}} \quad \text{cylinder}$$

$$C_f = \frac{1.33}{\sqrt{Re_\ell}} \quad \text{flat plate}$$

} laminar (4.22)

Let us take

$$C_f = \frac{K}{\sqrt{Re_\ell}}$$

then

$$a = \frac{Re_\ell}{2}\left[\frac{\sigma}{K\,q\,D}\right]^2$$

$$\sqrt{\frac{a}{C_f}} = \frac{(Re_\ell)^{3/4}}{\sqrt{2K}} \quad \frac{\sigma}{K\,q\,D}$$

and

$$C = \left[\frac{Re_\ell}{K^2}\right]^{3/4} \frac{\sigma}{\sqrt{2}\;\; q\,D} \qquad (4.23)$$

Re_ℓ = local Reynolds number at the shoulder

K = constant

σ = surface tension in pounds per inch

q = free stream dynamic pressure in pounds per square inch

D = drop diameter in inches

This permits the drop breakup time to be written as

$$t_b = \left[\frac{\sqrt{Re_\ell}}{K} \right]^{3/2} \frac{\sigma}{\sqrt{2}\ q\ D} \frac{D}{V} \sqrt{\frac{\rho_w}{\rho_a}}$$

Using dimensionless quantities we obtain

$$\sqrt{2\ K^3} = (Re_\ell)^{3/4} \left[\frac{\sigma}{q\ x_b} \right] \left[\sqrt{\frac{\rho_w}{\rho_a}} \right] \qquad (4.24)$$

where

x_b = breakup distance in inches

For two different stagnation pressures, p_{t_1} and p_{t_2}, we will get two breakup distances, X_{b_1} and X_{b_2}.

Forming a ratio for these two conditions from Eq. (4.24), we get

$$Re_\ell \propto p_t$$

$$q \propto p_t$$

$$\rho_a \propto p_t$$

σ, ρ_w, K, are constants. Thus

$$1 = \frac{(p_{t_2})^{3/4}}{(p_{t_1})^{3/4}} \frac{(p_{t_1})}{(p_{t_2})} \frac{X_{b_1}}{X_{b_2}} \frac{(p_{t_1})^{1/2}}{(p_{t_2})^{1/2}}$$

and

$$\frac{X_{b_2}}{X_{b_1}} = \left[\frac{p_{t_1}}{p_{t_2}} \right]^{3/4} \qquad (4.25)$$

Thus the stagnation pressure is seen to be a convenient parameter to vary in a wind tunnel test of the equations that describe the water drop breakup process.

In addition to Eq. (4.19), the following qualitative information about the drop breakup process has been obtained from the literature surveyed.

1. The "breakup time" for the drops is strongly dependent upon the relative velocity.
2. Final drop size (after breakup) is quite likely on the order of 10 microns as compared with an initial drop diameter of 2000 microns.
3. For supersonic relative velocity, the breakup distance (relative velocity multiplied by the "breakup time") will almost certainly be a foot or less and probably will be considerably less than a foot.
4. Viscosity and surface tension effects are unimportant compared to drag forces at the speeds under consideration.

Based on the preceding information on drop breakup, MITHRAS has proposed to utilize a flow separation spike extending upstream of the radome to produce a region of relatively high velocity (with respect to raindrops). (See Fig. 7.)

The separated boundary layer from the spike in front of the body produces a trapped-air region in front of the body as indicated in Fig. 7. This trapped-air region possesses a velocity with respect to on coming raindrops of approximately the missile velocity. In addition, the air between the oblique shock and the trapped-air region possesses a velocity with respect to the oncoming raindrops that is fairly high. The raindrop, in traversing both flow fields, will be quickly broken up into a fine mist before it can reach the missile nose. A discussion of the aerodynamic behavior of spike-tipped radomes which may be found useful is contained in Ref. 39. In addition, a considerable body of additional literature on spiked-bodies exists but has not been referenced in the interests of brevity and because the aerodynamic design and performance of spiked-bodies is not under consideration in this report.

The effect of particle or drop impact on various materials has been investigated by several authors. While the relations describing damage due to drop impact have not been completely determined, it would appear that for solid particles, the particle penetration is nearly proportional to the particle diameter (see Eq. 3.1). By breaking the raindrop up into much smaller drops, the damage due to individual impacts is considerably reduced and the effect of the individual impacts are spread over the entire radome surface rather than being concentrated at particular points. The total overall damage will be much less for the protected radome than for the unprotected radome.

The amount of protection afforded the radome by the presence of a protruding spike depends upon the spike length. If the spike is too short, the radome will be eroded because the water drops will have impacted the radome before they have had time to disintegrate. If the spike is made too long, aerodynamic difficulties are encountered.

The proper spike length can be calculated from Eq. (4.19) by inserting the desired value of drop diameter and missile flight conditions. Reference to literature on spiked-bodies will then indicate whether the spike length is aerodynamically acceptable. It should be noted at this time that the requirements on spike design imposed by erosion resistance considerations, i.e., spike length, are generally compatible with the aerodynamic requirements on the spike design.

5. TEST EQUIPMENT

The successful investigation of the rain erosion problem and the determination of the solution to this problem require that studies be carried out under controlled conditions. For this purpose, MITHRAS has been constructing an erosion simulation system to produce high velocity water drops in a supersonic air stream. This system will permit the study of the basic erosion process, material resistance to erosion, water drop behavior in supersonic airstreams, and proposed erosion alleviation methods. The erosion simulation system consists of three main components; the air channel to produce a supersonic airstream (table 1 contains a summary of the typical operating parameters of the channel), the water injection system to produce the high velocity water drops, and the photographic system to determine drop velocity and, if possible, to record the erosion process and drop breakup phenomena.

By injecting a jet of water into the airstream of a supersonic wind tunnel at a velocity slightly different from the stream velocity, it is expected that the jet can be made to break up into drops of known size. This stream of drops can then be directed at components and models of missiles and airplanes to simulate the flight of the missile through a rainstorm.

Reference 35 indicates that the following relation may be used to predict the final drop size resulting from the jet breakup.

$$X = \left[\frac{\sigma_w}{\rho_A \cdot V^2}\right] 0.60 \left[\frac{\mu_w V}{\sigma_w}\right]^{\frac{2}{3}} \left[1 + \frac{10^3 \rho_a}{\rho_w}\right] \left[\frac{D_j \rho_w \sqrt{v \sigma_w \mu_a}}{\mu_w^2}\right]^{\frac{1}{6}} \quad (5.1)$$

where

X final drop diameter

σ_w surface tension of the drop

ρ_a airstream density

Table 1. Mach Number 2.0 Erosion Simulator Characteristics

p/p_t	= 0.1278	p_{t_1}	= 25.56 psi
ρ/ρ_t	= 0.2300	p_1	= 3.267 psi
T/T_t	= 0.5556	T_t	= 530° R (70° F)
q/p_t	= 0.3579	T_1	= 294° R (−166° F)
A/A^*	= 1.688	p_2	= 14.7 psi
v/a^*	= 1.63299	p_{t_2}	= 18.43 psi
M_2	= 0.5774	T_2	= 496° R (36° F)
p_2/p_1	= 4.500	a	= 841 ft/sec
ρ_2/ρ_1	= 2.667	U	= 1682 ft/sec
T_2/T_1	= 1.688	q	= 9.148 lb/in^2
p_{t_2}/p_{t_1}	= 0.7209	A	= 10 in^2
p_1/p_{t_2}	= 0.1773	A^*	= 5.924 in^2
		ρ_{t_2}	= 0.004047 $\frac{sl}{ft^3}$ (0.1295 $\frac{lb}{ft^3}$)
		ρ_1	= 0.0009308 $\frac{sl}{ft^3}$ (0.02979 $\frac{lb}{ft^3}$)
		ρ_2	= 0.002482 $\frac{sl}{ft^3}$ (0.07945 $\frac{lb}{ft^3}$)
		Re/ℓ	= 6.594 x 10^6 ft^{-1}
		$\dot{m}$	= 3.48 lb/sec (c 108 sl/sec)
		P_{H_2O}	= 19,000 psi

Note: The symbols used in this table are identical with those used in Reference 47.

ρ_w drop density

V relative velocity between jet and air

D_j jet diameter

v jet velocity

μ_w viscosity of drop

μ_a viscosity of airstream

By rearranging the equation, the jet diameter and jet velocity may be computed when the drop size is specified.

Using the familiar Bernoulli equation, an estimate of the required pressure for a given jet velocity can be readily obtained (Fig. 8). The Bernoulli equation is

$$p \cong \frac{1}{2} \rho v^2 \qquad (5.2)$$

where

p jet supply pressure

ρ density of water

v velocity of jet

Compressibility effects will affect the answer somewhat but as shown in Fig. 8, these effects are small. The required velocity of the jet is approximately equal to that of the airstream into which injection is occurring. For a Mach number of 2 with a stagnation temperature of 70° F, the isentropic perfect gas relations give an airstream velocity of 1682 ft/sec. The pressure required to produce this velocity is found from Eq. (5.2) to be 19,000 psi.

Equation (5.1) and Ref. 35 show that the final drop size in an atomizing jet is to a large extent unaffected by injector diameter, injection velocity, and injector orientation (with respect to the airstream). Thus the controlling parameter is relative velocity and the final drop

size is effectively determined by this parameter and is independent of the other parameters. Furthermore, in the tests reported (Ref. 35), at distances from the jet nozzle greater than one foot, the drop size was approximately constant. It, therefore, appears possible to control drop size and distribution by adjusting the water jet velocity (and thereby the relative velocity between the jet and the airstream) through a range from slightly greater, to slightly less than the test section airstream velocity. Based on the results obtained in Ref. 35, it is expected that drop diameter will vary as the relative velocity to the minus four-thirds power or the jet supply pressure to the minus two-thirds power. This would imply that the requirements on controlling the jet supply pressure are not severe.

5.1 Erosion Simulator

Figure 9 shows, schematically, the Mach 2 blow-down erosion simulator that is under construction to determine the destructive effects of high velocity water drops on materials used in flight vehicles. The water pump, accumulator, and valving shown in Fig. 10 will be used with this tunnel. The water nozzles and materials holder will be similar to those shown in Figs. 22, 26, and 27.

For a general description of blow-down wind tunnels and its elements, refer to Ref. 40 and for the design of wind tunnels and pressure systems, refer to Refs. 40, 41, and 42.

The erosion simulator is designed to operate with a stagnation temperature of 560° R and a stagnation pressure ranging up to 60 psi. Air storage equipment and the air compressor are expected to provide a capability of 20 to 30 runs per day with a stagnation pressure of 30 psi and a run time on the order of 10 seconds. Since actual testing time is on the order of 2 seconds, this run time should be more than sufficient.

The photographic system to be used with the simulator has dictated that large viewing windows be provided as indicated in Fig. 9. It is expected that the tester will accommodate a 1/2" x 1/2" square model. Access ports for the water injection system are not indicated in Fig. 9 but these are located 90° around from the p_0 and T_0 instrumentation port in the stilling section.

5. 2 Water Injection System

The water injection system is required to pump water to a pressure of several thousand psi, store it, and then release it rapidly into a supersonic airstream at a velocity approximately equal to that of the airstream. The injection system is shown schematically in Fig. 10.

The pumping unit used is a Sprague* S-440 ready-to-use-pump unit with an S-216-C-300 basic pump. "The pump is an air driven reciprocating pump, identical in operating principle to the conventional stream-driven cylinder pump. Through a 4-way valve, air pressure is introduced on one side of a piston at the same time the other side of the piston is vented to exhaust. At the opposite end of the shaft is connected a liquid end piston which receives the undiminished force developed by the air piston and transforms this force into liquid pressure.

"Since the force transmitted is the same for both liquid and air pistons, the pressure developed on the liquid side is inversely proportional to the ratio of the piston areas. Thus when 100 psi air is used to operate a S-216-C-300 pump, which has a nominal ratio of 300: 1, the liquid pressure will be approximately 300 x 100, or 30,000 psi." (See Ref. 43.) This unit has a maximum pumping rate of approximately 0.1 gpm.

The pump output pressure is read from a Marshalltown 30,000 psi gauge. This unit has an accuracy of 1/2 percent of full scale or 150 psi.

The quick-opening valve is an Aminco** type 44-5912 Quick-Opening Valve. (See Ref. 44.) This unit is reported by the manufacturer to go from full closed to full open in 4 or 5 milliseconds.

The remaining components of the water injection system, with the exception of the jet nozzles, are standard Autoclave*** hardware (30,000 psi, stainless steel) and a description of these components may

* Sprague Engineering Corporation, Gardena, California
** American Instrument Co., Inc., Silver Spring, Maryland
*** Autoclave Engineers, Inc., Erie, Pennsylvania

be found in Refs. 45 and 46. Special mention deserves to be made of the accumulator.

This unit is a cylinder with a 2-liter capacity. It is made from stainless steel and is designed to operate with an internal pressure of 30,000 psi. The unit has pressure fittings at either end; the top fitting accommodates the nitrogen input system and a safety blowout disc; the bottom fitting accommodates the water input and outlet systems.

The operation of the water pumping system is as follows. With valve 5 closed, tap water is admitted from valve 6 and after filtering reaches the Sprague high pressure pump. With valves 1, 2, 4, and 11 closed and 3 open, the high pressure water on the outlet side of the pump is admitted into the 2-liter pressure vessel or accumulator. Valve 1 serves as a safety valve in the event of failure of valve 2 which is a special quick-opening valve. By first opening valve 1 and then valve 2 the high pressure water in the accumulator is quickly released and after passing through a suitable nozzle this water emerges as a supersonic jet. In practice, valve 3 is closed prior to the opening of valve 2. This prevents the needle in the high pressure gauge from slamming into its stop upon the sudden release of pressure in the system. Valve 4 serves the dual purpose of providing a bleed for the high pressure water and is also used in filling the accumulator with water. This is accomplished by connecting valves 4 and 5 with a length of tygon tubing. Valves 3, 4, 5, 11, and 9 are opened and water enters through valves 6, 5, 4, and 3 in that order. Valves 1 and 2, of course, remain closed. Displaced air escapes from the accumulator through valves 9 and 10.

Because of the small compressibility of water, only a small volume change is required to bring the water back to atmospheric pressure and the duration of the supersonic jet is therefore quite short. In some cases it may be required to have fairly long jet durations. This is possible if pressurized gas is used in the accumulator. This gas, because of its large compressibility, then serves as a spring and greatly increases the jet duration. For this purpose, provision is made in the water injection system for introducing 2300 psi nitrogen into the accumulator through

valves 10 and 11. After valves 10 and 11 are closed, the system is then pumped up with water, compressing the nitrogen until the required pressure is reached.

Valves 7 and 8 are used to control the flow of 100 psi driving air into the pump and thereby control the pressure at the high pressure side of the pump.

The operating parameters of the water pumping system are determined largely by the jet or water drop velocity desired. In all calculations to date, the required velocity has been taken to be 1682 ft/sec or Mach 2 at a stagnation temperature of 70° F. The pressure required to produce this velocity can be quite accurately determined from Bernoulli's equation. This relation is plotted in Fig. 8 where the design pressure, for a lossless system, is found to be 19,000 psi. For computational ease, this pressure will be considered to be 20,000 psi.

The compressibility of water is approximated by

$$\text{compressibility} = X = \frac{C}{L + P} = \frac{\Delta V/V}{\Delta P} \qquad (5.3)$$

where C and L are constants and P is the pressure. At the pressure level considered (20,000 psi), X is nearly constant at about

$$3.5 \times 10^{-11} \frac{\text{cm}^2}{\text{dyne}} = 2.42 \times 10^{-6} \frac{\text{in}^2}{\text{lb}}$$

(See Ref. 36.) This allows us to plot ΔP versus $\Delta V/V$ as in Fig. 11. From this figure we find that the fractional volume change amounts to five percent for ΔP of 20,000 psi.

Figure 12 plots usable volume required versus flow time for various standard tubing sizes (four right hand lines) and 0.040" i. d. restricted tubing (this latter tubing can be made from standard tubing by adding a nozzle with an 0.040" throat). It must be noted that Fig. 12 assumes constant pressure. By using Fig. 11 in conjunction with Fig. 12, the total volume required can be found.

If a gas is first introduced into the accumulator of the water injection system and water is then pumped in until the required pressure is reached, then the gas will act as a spring (because of its large compressibility) and permit longer run times for the same accumulator volume and pressure drop.

Because of their low solubilities and cost, helium and nitrogen gas were considered for use as the charging gas. Nitrogen was selected because of its lower cost (1/4 that of helium) even though it is somewhat more soluble than helium (2-1/2 times). By introducing the nitrogen into the accumulator at nominal storage pressure (approximately 2,000 psi), it becomes necessary to compress the gas by a factor of only 10.

Assuming that the gas temperature remains constant at 560° R and that the perfect gas law holds, we have

$$p = \rho R T \tag{5.4}$$

Also

$$\rho = \frac{m}{V} \tag{5.5}$$

where

m is mass of the gas

V is the volume of the gas

If no gas is allowed to escape from the accumulator, i.e., the gas remains in the upper portion of the accumulator while the water in the lower half leaves through the bottom fitting, then m is a constant and we can write

$$m = a\ V_0\ \rho_{2000} \tag{5.6}$$

where

a is the fraction of the accumulator volume occupied by the gas at 2,000 psi

$\rho_{2,000}$ is the gas density at 2,000 psi

Thus

$$p = \frac{a V_0 \rho_{2,000}}{V} R T \tag{5.7}$$

and

$$\Delta P = - \frac{a V_0 \rho_{2,000} R T \Delta V}{V^2} \tag{5.8}$$

at P = 20,000 psi, we have

$$\Delta P = - \frac{a V_0 \rho_{2,000} R T \Delta V}{\left[\frac{a V_0}{10}\right]^2}$$

$$\Delta P = - \frac{100 \rho_{2,000} R T \Delta V}{a V_0} \tag{5.9}$$

This relation is plotted in Fig. 13. As an example, let the flow time be 0.02 seconds with a nozzle diameter of 0.040". From Fig. 12 ΔV = 0.5 cubic inches. If ΔP is taken as 250 psi, then from Fig. 13, for a = 1, V_0 = 400 cubic inches.

The water injection system that has been built is designed to operate at a jet velocity of approximately 1600 feet per second. This unit can be used up to velocities of perhaps 1900 feet per second, but for velocities greater than 2000 feet per second it will be necessary to construct another higher pressure unit. With currently available hydraulic pumping equipment, velocities in excess of 3,500 feet per second are attainable.

5.3 Photographic Instrumentation

The photographic system is used to determine the velocity of the water drops in the supersonic airstream.

The system (Fig. 14) consists of two cameras, two electronic flash units, two electronic time delay circuits, a trigger circuit, and a switch.

This arrangement was used in order to obtain two individual

silhouette photographs of the subject with a known time interval between each exposure. The images are separate, distinct photographs rather than the conventional superimposed double exposure technique. The cameras, light sources, light baffle, and translucent screen are arranged in a manner that allows the No. 1 camera to receive illumination only from the No. 1 light source and the No. 2 camera to receive light only from the No. 2 light source.

The cameras are conventional "Speed Graphics" with "Polaroid" adaptors. The light sources are ten microsecond flash duration, four watt second energy units.

The electronic trigger circuit and delay circuits were designed and constructed by personnel at MITHRAS.

The photographic system is operated in the following manner. The trigger switch is activated when the quick opening valve is operated. This energizes the trigger circuit which activates the No. 1 delay circuit. The No. 1 delay is an adjustable electronic time delay circuit with an operating range from 10 μ sec to 1 second. The purpose of this circuit is to allow enough time for the water to flow through the valve, plumbing, injection nozzle, and into the field of view of the No. 1 camera. During the wind tunnel tests this time interval was usually set for approximately 1 millisecond. The output pulse from the No. 1 delay unit activates the No. 1 flash unit, producing the first exposure on the No. 1 camera and simultaneously energizes the No. 2 delay circuit. The purpose of the No. 2 delay unit is to allow a known time interval between exposures in order to determine water velocity and characteristics of the water jet with time. The No. 2 delay circuit is a "one shot multivibrator" with an operating range from 5 μ sec to 1 second. For the wind tunnel tests this time interval was adjusted to allow the water to move approximately 2 inches between exposures which was a delay of approximately 100 μ sec between flashes. At the end of this delay the No. 2 flash unit is activated which produces the exposure on the No. 2 camera.

A Tektronix model 551 oscilloscope is used to set the time delays initially and on each test the time interval between exposures is photographed

with an oscilloscope camera. The "synchronous" pulse starts the sweep of the oscilloscope and the output from each delay circuit then produces a pulse on the cathode ray tube.

During a typical "run" all camera shutters are set for one second and ambient room illumination on the translucent screen is reduced to a level that does not fog the film. All shutters are opened simultaneously with solenoids and the quick opening valve is then operated approximately 1/2 second later The quick opening valve operates the trigger switch which starts the sequence described above. At the end of one second all camera shutters are closed, the system is turned off, and the Polaroid film is then inspected for results.

The triggering switch consists of two leaves of brass shim stock, insulated from each other as shown in Fig 15. The switch is placed between the cam-follower stop and the valve base when the valve is in the cocked position. When the cam is rotated, the cam follower and cam-follower stop drop, forcing the two brass leaves into contact, thereby completing the electrical triggering circuit. Figure 15 shows the valve in the cocked position with the switch mounted between the cam-follower stop and valve base.

5. 4 Model

The test model upon which erosion effects are measured consists of a hollow transparent tube with the downstream end closed by the target material. This tube can be either rectangular or circular in cross section. Aerodynamically, the upstream or open end of the tube appears to be closed since the air within the tube is at stagnation conditions Thus water drops must traverse the dead-air or stagnation region in the tube before they can impact on the target. The separated flow region produced by spike tipped bodies is thereby simulated in this manner

5. 5 Check Out of Equipment and Preliminary Study of Jet Behavior in Partial Vacuums

In order to check out the photographic and water injection systems and at the same time study the behavior of high speed water jets in low

density air (on the order of 1-1/2 psi which approximates the static pressure in a Mach 2 wind tunnel at a stagnation pressure of 1 atmosphere), a 4-foot length of 4-inch i.d. pyrex tubing was placed in front of the water injection nozzle and partially evacuated (see Fig. 16). Thin brass stock (0.001 to 0.003 inches thick) was selected as the target since drop impacts would produce permanent dents in this material. The photographic system previously described was set up to record the water injection process and to provide jet velocity measurements.

Several tests were made to determine the erosion effect of the high speed water. Severe damage was noted to nearly all samples ranging from denting of the surface to complete shredding of the sample. Water velocity, as measured by the photographic system, was found to be about 1,000 ft per second for a 12,000 psi supply pressure (distance from the nozzle to the point photographed was approximately 2 feet). Runs at supply pressures up to 30,000 psi were successfully made but no velocity data on these runs was obtained.

Much valuable information was gained from these tests. From an examination of the target samples it was immediately apparent that large quantities of water drops were produced at distances from the nozzle on the order of 2 to 3 feet. These drops produced dents in the target material (0.003 inch thick brass shim stock) that were on the order of 0.05 inches in diameter. It also was noted that the drops appeared to be formed in an annular region about a central solid jet (see Fig. 17), as evidenced by the fact that the target was punctured on the jet center line. Thus a damage pattern of the form shown in Fig. 17(a) was produced. This agreed with the data given in Ref. 34. In order to obtain information on the damage produced by water drop impacts rather than jet impact it became necessary to position the target off the jet axis so that only water drops impacted the target material (see Fig. 18). For this reason a moderately thick piece of brass with a circular aperture was placed before the target to prevent its destruction by the solid portion of the water stream.

Of considerable interest was the fact that jet breakup was increased by changing the ambient pressure from atmospheric to partial vacuum (80 mm of mercury). At this time the only reason suggested for this jet behavior is the possibility that dissolved air escapes from the jet, at the low ambient pressure, and thereby accelerates the jet breakup process.

Because of the convenience of this Pyrex tube, i.e., transparent sides for photographing the high speed water, easy access to target and water nozzle, it is anticipated that further tests will be made in this device. It appears to be particularly well suited for checking out system components and for material testing studies prior to installation in the MITHRAS erosion simulator.

6. SYSTEM TESTS AT GAS TURBINE LABORATORY (Massachusetts Institute of Technology)

During the period of September 7 through September 18, 1962, tests were conducted at the Gas Turbine Laboratory (GTL) of the Massachusetts Institute of Technology (MIT). The MITHRAS water injection system, drop-breakup model and the MITHRAS velocity measuring photographic system were installed in the Mach 2 GTL supersonic facility.

The availability of this Mach 2 wind tunnel at the GTL presented the opportunity both for immediate testing of the water injection system and also of an early determination of the feasibility of the proposed MITHRAS solution to the rain erosion problem. It was anticipated that such tests could provide immediate preliminary data and experience which would be of great value in further tests to be conducted in the MITHRAS blowdown "erosion simulator."

The GTL tunnel is a continuous circuit vertical tunnel designed to operate in the low supersonic flow regime. The test section is located in the "up" leg of the tunnel and measures 8 inches by 8 inches (see Fig. 19). The nozzle blocks used in these tests provide Mach 2 flow over a range of stagnation pressures and temperatures. The wind tunnel walls, from the stilling section to the downstream end of the test section, are formed by flat doors on either side of the tunnel. The doors used in this test were made of flat pyrex glass so that it was possible to photograph through the tunnel over the entire region from the stilling section to the diffuser (see Fig. 20). Use of these glass doors was most advantageous since it permitted the injected water to be photographed from the point of injection, near the wind tunnel throat, to the point of impacting on the model target, at the aft end of the test section.

Figure 21 shows the GTL tunnel with opened door. The sleeved model and injection nozzle are visible in the tunnel. The water injection

system is seen to the left of the tunnel with the nitrogen supply bottles (which were not used) next to the water pumping system. Just to the left of the nitrogen bottles are located the time delay and triggering equipment and the oscilloscope and camera used to display the electronic timing signals.

6.1 Water Injection System

The water injection system used in the GTL tests is the same system that will be used in the MITHRAS erosion simulator. Nitrogen gas was not used during the GTL tests because:

1. The photographic equipment did not require long run times.
2. Visible target damage was obtained without the employment of the pressurized gas.
3. It was desired to keep the amount of water introduced into the GTL tunnel to a minimum, both to minimize its effect on the tunnel compressor and to keep as much water as possible off the pyrex doors so that photography would not be hampered.
4. Time limitations made it advisable to concentrate on other more important phases of the test program.

The water injection system was mounted on a steel bench and access into the tunnel was made through a hole provided.

The nozzle support arrangement is illustrated in Fig. 22. Three configurations were provided so that the nozzle exit location could be varied. A coupling employing either a 6" or 4" nipple could be inserted between the nozzle and the tee connector for 2 configurations while the nozzle could be coupled directly to the tee connector for the third configuration. By using these three different configurations, the nozzle exit location could be varied over a distance of nearly 7 inches. This variation was provided because of the total lack of information on jet breakup

under the conditions which were to be run. Photographs of the three configurations are shown in Figs. 23, 24, and 25.

6.2 Water Injection Nozzles

It was intended that three different water injection nozzles would be tested. Because of time limitations only two nozzles were actually tried.

The three nozzles were constructed in identical fashion. A five inch length of 1/4" x 0.083" stainless steel tubing was silver-soldered into a 10-1/2 inch length of 9/16" x 3/16" stainless steel tubing and the plug containing the nozzle contour was then silver-soldered into the tip of the smaller tube (see Fig. 26). The three nozzle contours are shown in Fig. 26. The first five test runs were made with nozzle No. 2 at which time it was noted that the plug containing the nozzle contour had been blown from the nozzle. Reference to the photographs of the previous runs indicated that the nozzle plug was lost during the third test run. For the remainder of the test schedule, nozzle No. 1 was employed.

6.3 Model

The wind tunnel model was designed so that the effectiveness of a flow separation region in breaking up water drops could be determined. For this purpose, the model illustrated in Fig. 27 was built. The target support and sleeve support were mounted on the GTL sting which is permanently mounted in the aft end of the test section and is capable of axial variation of position. A target (thin sheets of brass), an aperture (to confine erosion to a small area of the target), and a retaining ring are fastened to the target support as shown in Fig. 27. A 1-3/4" o.d. x 1-1/2" i.d. plexiglass sleeve can be mounted to provide a still air region in front of the target as shown in Fig. 28. This dead air region thus simulates the separated flow region which is produced by a spike mounted in front of a radome in supersonic flow. Several tube lengths were available but most runs employing the sleeve were made with a sleeve that extended six inches upstream from the target. Calculations

indicated that this sleeve length was sufficient to induce water drop breakup (see Appendix A).

During some runs clay was used to back the target to provide support. This was done to prevent target rupturing during wind tunnel starting. Some unbacked targets were lost during wind tunnel starting. The clay backing, because of its plasticity, did not impair target indentation upon water drop impact and proved quite satisfactory as a backing material.

An exploded view of the model is provided in Fig. 29 and Figs. 23, 24, and 25 show the model installed in the GTL tunnel. In Fig. 23 the model is located in the extreme downstream position while in Fig. 24 the model is mounted in the extreme upstream position.

6.4 Photographic System

The photographic system used in the GTL tests was identical to the one previously described in section 5.3. However the cameras and light sources used in the GTL tests were arranged side by side rather than in a vertical plane since the GTL tunnel test section is vertical (see Fig. 20).

The photographic system was used to determine the velocity of the injected water in the GTL tunnel. Although the system was not designed for the purpose of resolving water drops, the test photographs were examined in an attempt to locate individual water drops. These attempts were, unfortunately, unsuccessful.

It was only after the MIT tests were completed that equipment for calibrating the photographic light sources became available. It was hoped that these light sources would have a 1 micro-second flash duration. At water velocities of 1682 ft per sec, the displacement during the flash duration would be 0.02 inches. Figure 30 shows the result of the light source calibration. In part (a) the oscilloscope trace of the light source output is shown. The time scale is 5μ seconds per large division. It can readily be seen that the pulse duration is on the order of 10 μ seconds which produces a displacement of 0.2 inches during the

flash duration. This produces blurring as evidenced in part (b) of Fig. 30 which is a photograph of a bullet travelling at approximately 1145 ft per sec taken with the photographic system used during the GTL tests.

With such a long flash duration there can be no hope of discerning individual drops which are travelling at an appreciable velocity and it is therefore not surprising that individual water drops were not detected in the test photographs.

6.5 Run Schedule

The pre-run schedule for the wind tunnel program at MIT included provisions for

1) testing the three different nozzle configurations for
   a) formation of drops
   b) drop velocity
2) determining jet breakup distance
3) determining the effect of static air density on the drop breakup distance, and
4) determining the feasibility of flow separating devices for protecting radomes from rain erosion

Because of various difficulties encountered during this first program, only the fourth objective was attained. This objective, however, was by far the most important.

In the original run schedule, four full days of run time were allocated for testing. Actual testing time, however, amounted to approximately one day.

Table 2 contains a summary of the test runs that were conducted at the GTL facility.

The test procedure used was identical to that described in sections 5.2 and 5.3 and proved quite satisfactory.

Table 2 RUN SCHEDULE

Run No	Water Pressure (psi)	Time to 1st Flash (milliseconds)	Time Between Photograph (Δt) (microseconds)	Nozzle No	Model Sleeve Length (inches)	Target Thickness (inches)	Target Aperture (inches)	Distance of Nozzle Tip from Tunnel Throat (in.)	Distance of Target from Nozzle Tip (inches)	Jet and Drops Photographed	Comments
0	-	-	-	-	0	-	-	2 13/16	13 8	No	
1	20,000	36	200	2	0	0 002	3/8	"	"	Yes	
2	20,000	25	200	2	3	0 001	1/4	"	"	No	No water in photographs
3	20,000	30	200	2	3	0 001	1/4	"	"	No	" " " " Water nozzle lost
4	20,000	34	200	2	3	0 001	1/4	"	"	Yes	Water nozzle lost
5	20,000	29 75	200	2	3	0 001	1/4	"	"	Yes	Water nozzle lost
6	20,000	34	200	1	6	0 001	1/4	"	"	Yes	New nozzle, slight denting of target
7	20,000	30	200	1	0	0 001	1/4	"	"	Yes	Moderate denting of target Minor puncture of target
8	20,000	29	200	1	6	0 001	3/8	"	"	Yes	No target damage
9	20,000	30	200	1	0	0 001	3/8	"	"	Yes	Moderate denting of target
10	21,000	20	200	1	0	0 001	3/8	"	"	Yes	Heavy target denting, target ruptured slightly
11	21,000	18	200	1	0	0 002	3 8	"	"	Yes	" " " " " "
12	20,000	23	200	1	0	0 001	3-8	"	"	Yes	" " " " " "
13	20,000	-	-	1	6	0 001	3/8	"	"	Yes	Scope not triggering, moderate target denting, minor puncture of target
14	20,250	-	-	1	6	0 001	3/8	"	"	Yes	Same comments as No 13
15	20,250	-	-	1	6	0 001	3/8	"	"	No	No photographs Same comments as No 13
16	20,500	17 5	100	1	6	0 001	3/8	"	"	Yes	Slight target denting
17	20,500	15. 5	100	1	6	0 001	3/8	"		Yes	Slight target denting
18	20,500	-	-	1	6	0 001	3/8	"	"	No	No photographs Slight target denting
19	20,000	15	220	1	0	0 001	3/8	"	"	Yes	Moderate target denting
20	20,000	10	220	1	0	0 001	3/8	"	"	Yes	" " "
21	20,000	-	-	1	0	0 001	3/8	"	"	No	No photographs Moderate target denting
22	20,000	8 1	100	1	0	0 001	3/8	4 13. 16	11 8	Yes	Moderate target denting
23	20,000	7 7	100	1	0	0 001	3 8	"	"	Yes	" " "
24	20,000	?	50	1	6	0 001	- 3/8	"	"	Yes	Water nozzle offset 1 16 inches Target destroyed
25	20,000	1	50	1	6	0 001	3/8	"	"	Yes	" " " " " " " "
26	20,000	1	50	1	6	0 001	3/8	"	"	Yes	" " " " " " " "
27	20,000	1	50	1	0	0 002	3/8	"	"	No	No water, safety valve closed Target destroyed
28	20,000	1	50	1	0	0 002	3/8	"	"	Yes	Target destroyed
29	20,000	1	50	1	0	0 002	3/8	"	"	Yes	" "
30	20,000	1	10	1	0	0 002	3/8	"	"	Yes	" "
31	21,000	1	10	1	0	0 005	3/8	"	"	Yes	Target supported by clay backing, target severely dented
32	21,000	1	10	1	0	0 005	3/8	"	"	Yes	Target supported by clay backing, target severely dented
33	21,000	1	10	1	0	0 005	3/8	"	"	Yes	Target supported by clay backing, target severely dented No 1 camera did not fire
34	21,000	1	10	1	0	0 005	3/8	"	"	Yes	No 1 camera did not fire No target
35	21,500	1	50	1	0	0 002	3/8	- 2 1/8	23 3/8	Yes	No 2 camera did not fire Severe denting of target, target ruptured, clay backing for target
36	21,500	1	50	1	0	0 002	3/8	"	"	Yes	Same comments as No 35
37	21,500	1	50	1	6	0 002	3/8	"	"	Yes	No visible damage, clay backing for target
38	21,500	1	50	1	6	0. 002	3/8	"	"	Yes	No 1 camera did not fire No visible damage, clay backing for target
39	-	-	-	-	0	0 002	3/8	"	"	No	Clay backing for target, check for tunnel particles, slight scratching of target

CONFIDENTIAL

6.6 Data Obtained

The data obtained in the GTL tests consisted of photographs of the injected water stream and the brass target samples used during each run.

The photographs of the injected water were similar to Figs. 31 and 33. However, in many cases, primarily during the earlier runs, no discontinuities in the jet were present, and velocity measurements were therefore not possible. Figures 32 and 34 are typical of the timing mark photographs that were taken of the oscilloscope. These photographs are used to determine the time interval between photographs.

In Figs. 31 and 33, the distance traversed by the water jet between photographs was obtained by measuring the distance moved by the discontinuities from some convenient reference point, either the tip of the water injection nozzle or the upstream end of the plexiglass sleeve on the model. The magnification of each photograph was determined by measuring some known distance, either the sleeve diameter (1.75 inches) or the diameter of the tip of the water injection nozzle (0.25 inches). The result of these velocity measurements is shown in Fig. 35. As is evident from Fig. 35, scatter in the data points is appreciable. This is primarily caused by:

1) poorly defined edges of the discontinuities
2) errors in determining the magnification of the photographs because of measurement inaccuracies
3) inaccuracies in measuring displacements of the jet discontinuities

The time interval measurements are expected to be much more accurate than the distance measurements.

Figures 36, 37, 38, and 39 are typical photographs of the brass targets retrieved after the test runs. Figure 36 shows the results obtained without the flow separating sleeve. The severe denting of the targets is quite evident.

In Figures 37, 38, and 39, the effect of the plexiglass sleeve is clearly shown. While some denting is present in the sleeved targets of Figs. 37 and 38, the severity of damage is less than in the unprotected targets. The sleeved target of Fig. 39, on the other hand, shows no damage at all while the unprotected target is severely damaged. The third target sample in Fig. 39 was used to determine the effect of small solid debris in the wind tunnel. As can be seen, the effect of such particles is quite minor.

Figure 40 is a photograph of a sample target that was used during the equipment checkout in the pyrex tube described in section 5.5. Figure 40 is included for comparison with Figs. 36 to 39. The damage to this target was identical in nature to that of the targets used in the GTL tests except that the indentations were slightly larger than those in the GTL targets. This has been taken to indicate that the drops in the GTL tests were slightly smaller than the drops produced during the equipment checkout.

It must be appreciated that photographs of the target samples lose considerable information from that obtainable with the original targets, however they do indicate the type and intensity of damage produced and also the effect of the flow separating sleeve.

6.7 Results of Tests at the Gas Turbine Laboratory

These preliminary and exploratory tests conducted at MIT's Gas Turbine Laboratory have led to the following results:

1. Drop formation from a jet of water which is traveling at supersonic velocity with respect to the ambient air takes place within 2 ft of the injection point at $M = 2$, $P_t = 14.7$ psi, $T_t = 560°R$.

2. Determination of water velocity by photographic means is feasible. Repeatability of the photographic system when triggered by the valve driven switch is excellent.

3. Use of thin sheets of brass as target materials to record drop impacts proved fairly reliable and provides permanent records of the water drop distribution and density.

4. Use of a dead-air region in front of the target, in general, reduced target damage. Protection ranged from fair to excellent.

The experience gained at the GTL facility indicates that the use of a closed-circuit erosion simulator may be undesirable because condensed water vapor in the tunnel air and water droplets on the windows can render photography impossible. In addition, some difficulty with the tunnel compressor was noted during and immediately after water injection. The open-circuit design of the MITHRAS erosion simulator is thus seen to be advantageous.

The long flash duration of the camera light sources used during these tests made it impossible to distinguish individual water drops on any of the photographs that were taken.

The photographs of the injected water that were taken during the early part of the injection process clearly show that a continuous jet is not produced initially. Rather a series of slugs of water are ejected. The reason for this is no doubt found in the dynamics of the injection system when subjected to the sudden application of a step change in water velocity or water pressure. The combined transients in the injection system and the liquid most likely produce the pulsations evident in the jet. At a later time in the ejection process these oscillations no longer appear, as evidently the transients have damped out.

A close look at Fig. 31 indicates that the water velocity decreases with increasing distance from the water nozzle. Since the airstream is at a velocity somewhat higher than that of the jet it would appear at first glance that the airstream would tend to accelerate the water. The reason for the deceleration of the jet is not certain although it has been proposed that the low velocity wake produced by the water injection nozzle and

associated hardware may be interacting with the injected water in such a manner as to produce a deceleration of the jet. This, however, remains to be proven.

The measured jet velocities as shown in Fig. 35 are some two to six hundred feet per second below the design velocity, depending upon the distance of the jet from the injection nozzle. The expected pressure losses in the system (as given in Appendix B) amount to some 3200 psi, which, when subtracted from a 21,000 psi supply pressure still should provide a velocity in excess of 1600 feet per second. Figure 35 indicates that the exit velocity may be somewhat less than the design velocity. This is quite possible in view of the rough character of the pressure loss calculations and also because erosion of valve and nozzle orifices may have significantly increased their friction coefficients. It should be noted that during repair of the quick-opening valve quite severe pitting of the valve stem was observed, necessitating the replacement of this part. The pits on this piece were estimated to be on the order of 1 mil deep. Roughness of this magnitude throughout the system could increase the system pressure losses to as much as 12,000 psi which corresponds to a jet velocity of 1150 feet per second.

6.8 Recommendations for Future Experiments

While the MIT tests have indicated that radome protection from rain erosion is afforded by the use of flow separation devices, many questions still remain to be answered. At the present time the validity of the drop breakup equation has not been experimentally substantiated. No attempt was made during the MIT tests to study the effect of varying the stagnation pressure of the supersonic airstream and consequently the variation of drop breakup distance with this parameter was not observed. It must be noted, in fact, that the drop breakup distance, for the test conditions, was never determined. This was caused by the short period of time available for testing and inadequate resolution capability of the photographic system. Therefore, one of the prime objects of future testing will be the experimental study of the drop breakup

equation, for without experimental substantiation of this relation, the design of erosion reducing flow separation spikes by the use of this equation is a questionable procedure.

While the brass targets retrieved from the model showed that protection against erosion was afforded by use of the plexiglass sleeve, complete protection was not obtained in all cases as evidenced by Figs. 37 and 38. It will therefore be necessary in future tests to determine what conditions are necessary to produce total protection. In particular, the effect of varying sleeve length will be closely examined.

The target material in the tests conducted was chosen to be brass shim stock because of the ability of this material to retain the indentations produced by the impacting water drops and thereby leave a permanent record of the water drop distribution. The effect of the water drop impact on typical radome materials, both with and without the plexiglass sleeve, at present cannot be inferred from the damage to the brass material. Samples of radome materials will be used as targets in future tests. It may then be possible to relate the observed damage of the brass material to that of the radome material.

The characteristics of the water jet and drop behavior in the supersonic airstream still remain to be investigated. Of particular interest will be the effect of nozzle geometry, injection velocity, and ambient conditions on jet breakup distance, drop size, and the cross sectional distribution of the water drops in the water stream.

In order to obtain photographs of individual drops in future tests the photographic light sources will have their storage capacitors changed from 2μfd to 0.25μfd which brings the flash duration down from 10 microseconds to nearly 1 microsecond. This should allow the photographing of individual drops. The reduction in light energy caused by this change will be compensated for by the use of a lower f-number, i.e., larger lens aperture, on the cameras. During the GTL tests the cameras were operated at an f-number of f/32. It is estimated that, with the new capacitors, it will be necessary to operate at f/8.

Because of the difficulty experienced in obtaining accurate reference dimensions for scaling the measurements obtained from the photographs, future tests will employ reference markers located along the axis of the air channel to facilitate measurements from the photographs. In addition, the time interval between photographs will be increased.

No major changes in the 30,000 psi water injection system are contemplated since the performance of this system appeared to be quite satisfactory. Prior to future tests, it will be necessary to inspect all critical orifices in the water flow path to insure that excessive roughness is not present. This should increase the velocity of the injected water by approximately two hundred feet per second. The basic test model configuration used during this program will also be retained except that a variety of materials will be tested.

7. CONCLUSIONS

This report has covered research accomplished during the first year of a two-year program. A first round of tests has established the feasibility of the rain erosion control method proposed by MITHRAS Protection ranging from fair to excellent can be achieved. A large portion of the erosion simulator with its associated equipment has been constructed.

During the forthcoming year the erosion simulator will be completed with faster photographic equipment and an intensive test program will be conducted. Meanwhile additional tests in the large pyrex tube described in this report will also be conducted. These tests will cover the fundamental aspects of drop breakup and materials testing.

The research program for the new year will provide a firm basis for the intelligent design of spiked radomes that are relatively safe from the effects of high speed flight through rain.

8. REFERENCES

1. Aeroelastic Structures Research Laboratory. Proposal for a Coordinated Theoretical and Experimental Study of High Speed Impact and Penetration. Department of Aeronautics and Astronautics, School of Engineering, Massachusetts Institute of Technology (MIT), Cambridge, Mass., December, 1960

2. Bruntun, J. H. Deformation of Solids by Impact of Liquids at High Speeds. Paper presented at 64th Annual Meeting, ASTM, Atlantic City, New Jersey, June 29, 1961. Symposium on Erosion and Cavitation, ASTM Special Technical Publication No. 307, pp. 83-97.

3. Charters, A. C., Locke, Jr., C S A Preliminary Investigation of High Speed Impact: The Penetration of Small Spheres into Thick Copper Targets. NACA RM A58 B26.

4. Collins, Jr., R. D., Kinard, W. H. The Dependency of Penetration on the Momentum per Unit Area of the Impacting Projectile and the Resistance of Materials to Penetration NACA TN D-238.

5. DeCorso, S. M., Kothmann, R E. Erosion by Liquid Impact. Paper presented at 64th Annual Meeting, ASTM, Atlantic City, New Jersey, June 29, 1961. Symposium on Erosion and Cavitation, ASTM Special Technical Publication No. 307.

6. Engel, O. G. Waterdrop Collisions with Solid Surfaces. "Journal of Research of the National Bureau of Standards." Vol. 54, No. 5, May, 1955. Research Paper 2591.

7. Engel, O. G. Impact of Liquid Drops. Paper presented at 64th Annual Meeting, ASTM, Atlantic City, New Jersey, June 29, 1961. Symposium on Erosion and Cavitation, ASTM, Special Technical Publication No. 307

8. Fyall, A. A. Supersonic Rain Erosion Testing Using a Low-Cost Vehicle. Ohio State University. (SECRET)

9. Gibson, J. Testing of Rain Erosion Resistance of Aircraft Coatings. Applied Science Research Laboratory. University of Cincinnati, Navy Bureau of Aeronautics Contract NO. s 58-230d. Final Report, December 15, 1958.

10. Hurd, D. E., Holmes, R. F. A Study of Rain Erosion Testing Methods for Supersonic Speeds. Thermodynamic Laboratories, Convair, Wright Air Development Center, WADC TR 53-173, Part VI, January, 1960.

11. Istracon Report 60-1. Rocket Sled Design Handbook. January 1960.

12. Kinard, W. H., Lambert, Jr., C. H., Schryer, D. R., Casey, Jr., F. W. Effect of Target Thickness on Cratering and Penetration of Projectiles Impacting at Velocities to 13,000 feet per second. NASA Memo 10-18-58L.

13. King, R. B. Rain Erosion, Part IV. Royal Aircraft Establishment (Farnborough) Report No.: Chem 521, September, 1960, Ministry of Aviation, London, W. C. 2.

14. Lapp, R. R., Wahl, N. E. An Investigation of the Rain Erosion of Aircraft Materials at High Speeds. Cornell Aeronautical Laboratory, Inc., Buffalo, New York. Report No. PC-743-M-4, Monthly Progress Report, June-July, 1952. Wright Air Development Center Contract No. AF33(600)6469. E. O. R604-303-GR-7j, August 8, 1952.

15. Lapp, R. R., Thorpe, D. H., Stutzman, R. H., Wahl, N. E. The Study of Erosion of Aircraft Materials at High Speed in Rains. Cornell Aeronautical Laboratory, WADC TR 53-185, Part 4. November, 1957.

16. Plesset, M. S., Ellis, A. T. On the Mechanism of Cavitation Damage. Hydrodynamics Laboratory, California Institute of Technology, Pasadena, California. ONR Department of the Navy Contract N6onr-24420 (NR 063-059) Report No. 21-15, June, 1954.

17. Summers, J. L. Investigation of High-Speed Impact: Regions of Impact and Impact at Oblique Angles. NASA TN D-94.

18. Thompson, Jr., G. E. Testing of Rain Erosion Resistance of Aircraft Coatings. University of Cincinnati, Applied Science Research Laboratory, Progress Report No 1. October 1, 1959 to November 30, 1959, for Navy Bureau of Aeronautics, Contract NOas 60-6065-C, December 11, 1959.

19. Ungar, E. W. Investigation of High-Speed Particle Erosion of Melting Aerodynamic Surfaces. Battelle Memorial Institute, September, 1959. ASTIA AD 260 428.

20. Engel, O. G. Fragmentation of Waterdrops in the Zone Behind an Air Shock. "Journal of Res. of the Nat. Bur. of Standards." Vol. 60, No. 3, March 1958, Research Paper 2843.

21. Gordon, G. D. Mechanism and Speed of Breakup of Drops. "Jour. Appl. Phys." Vol. 30, No. 11, November, 1959. pp. 1759-1761.

22. Hanson, A. R., Domich, E. G. An Experimental Investigation of Air Blast Breakup of Liquid Droplets. "Proc. of 5th Biennial Tech. Conf." University of Minnesota, Institute of Technology., Department of Aero. Eng., Rosemount Aero. Labs., Research Report No. 137, October, 1956. pp. 57-61.

23. Hinze, J. O. Critical Speeds and Sizes of Liquid Globules. "Appl. Sci. Rev." Ser. A, Vol. I, No. 4, 1949. pp. 273-288.

24. Ingebo, R. D. Vaporization Rates and Drag Coefficients for Isooctane Sprays in Turbulent Air Streams. NACA TN 3265, Lewis Flight Propulsion Laboratory, Cleveland, Ohio, October, 1954.

25. Ingebo, R. D. Drag Coefficients for Droplets and Solid Spheres in Clouds Accelerating in Airstreams. NACA TN 3762, Lewis Flight Propulsion Laboratory, Cleveland, Ohio. September, 1956.

26. Lane, W. R. Shatter of Drops in Streams of Air. "Industrial and Engineering Chemistry." Vol. 43, No. 6, 1951. pp. 1312-1317.

27. Masugi, N. I. Theoretical and Experimental Study of the Deformation and Atomization of a Liquid Drop in a High Velocity Gas Stream. Paper presented at the American Rocket Society 11th Annual Meeting. Henry Hudson Hotel, New York, New York, November 26-30, 1956.

28. Morrell, G. Critical Conditions for Drop and Jet Shattering. NASA TN D-677, Lewis Research Center, Cleveland, Ohio. February, 1961.

29. Priem, R. J. Breakup of Water Drops and Sprays with a Shock Wave. "Jet Propulsion." October, 1957. p. 1084.

30. Wilcox, J. D., June, R. K. Apparatus for Study of the Breakup of Liquid Drops by High Velocity Airstreams. "Jour. of the Franklin Institute." Vol. 271, No. 2, March, 1961. p. 169.

31. Baron, Thomas. Atomization of Liquid Jets and Droplets. Engineering Experiment Station, University of Illinois, T. R. No. 4, February 15, 1949.

32. Dunne, B. Cassen, B. Some Phenomena Associated with Supersonic Liquid Jets. "Jour. of Appl. Phys." Vol. 25, No. 5, May, 1954. pp. 569-572.

33. Rupe, J. H. On the Dynamic Characteristics of Free Liquid Jets and a Partial Correlation with Orifice Geometry. Jet Propulsion Laboratory, California Institute of Technology, Pasadena, California. TR No. 32-207, NASA Contract No. NA 57-100. January 15, 1962.

34. Semerchan, A. A., Vereshchagin, L. F., Filler, V. M., Kuzin, N. N. Distribution of Momentum in a Continuous Liquid Jet of Supersonic Velocity.

35. Weiss, M. A., Worsham, C. H. Atomization in High Velocity Air Streams. Esso Research and Engineering Company, Linden, New Jersey. NOrd 16706, Bumblebee Series, Report No. 277, May, 1958.

36. Chemical Rubber Publishing Co. Handbook of Chemistry and Physics. 39th ed. Cleveland, Ohio. 1957-1958.

37. Schlichting, H. Boundary Layer Theory. McGraw Hill Book Co., Inc., New York, 1954.

38. Keenan, J. H., Kay, J. Gas Tables. John Wiley and Sons, Inc., New York, 1945.

39. Crawford, D. H. Investigation of the Flow Over a Spiked-Nose Hemisphere-Cylinder at a Mach Number of 6.8. NASA TN D-118, December, 1959.

40. Ferri, A., and Bogdonoff, S. M. Design and Operation of Intermittent Supersonic Wind Tunnels. Agardograph No. 1 Wind Tunnel and Model Testing, AD No. 20810.

41. ASME Boiler and Pressure Vessel Code, Section VIII. Rules for Construction of Unfired Pressure Vessels, 1959 Edition and 1959 Through 1961 Addenda. The American Society of Mechanical Engineers, 29 West 39th Street, New York 18, New York.

42. American Standard Code for Pressure Piping. ASA B31.1-1955, UDC-621. 64. 002. 1/. 2. The American Society of Mechanical Engineers, 29 West 39th Street, New York 18, New York.

43. Sprague Hydraulic and Pneumatic Equipment Bulletin No. 255 (Rev. B). Sprague Engineering Corporation, Gardena, California.

44. Superpressure Equipment Catalog 460. American Instrument Co., Inc., Silver Spring, Maryland, October, 1959.

45. Autoclave 30,000 psi Valves and Fittings Bulletin 555-B. Autoclave Engineers, Inc., Erie, Pennsylvania.

46. Autoclave Engineers Laboratory, Pilot-Plant, Plant Size Pressure Vessels, Bulletin 357-A, Autoclave Engineers, Inc., Erie, Pa.

47. Equations, Tables, and Charts for Compressible Flow. NACA Report 1135, Ames Research Staff, 1953.

48. Flow of Fluids Through Valves, Fittings and Pipes. Crane Technical Paper No. 410, Crane Company, Chicago, Illinois, 1957.

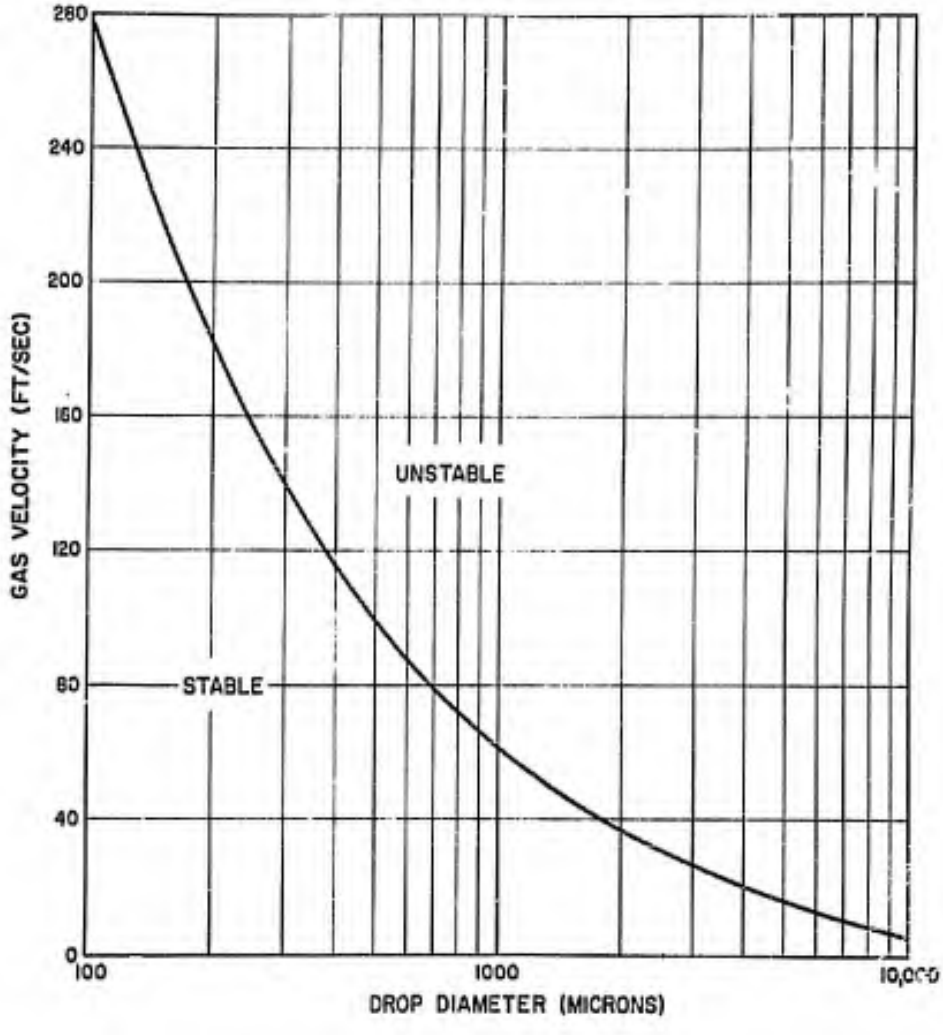

Figure 1. Critical velocity of water drops.

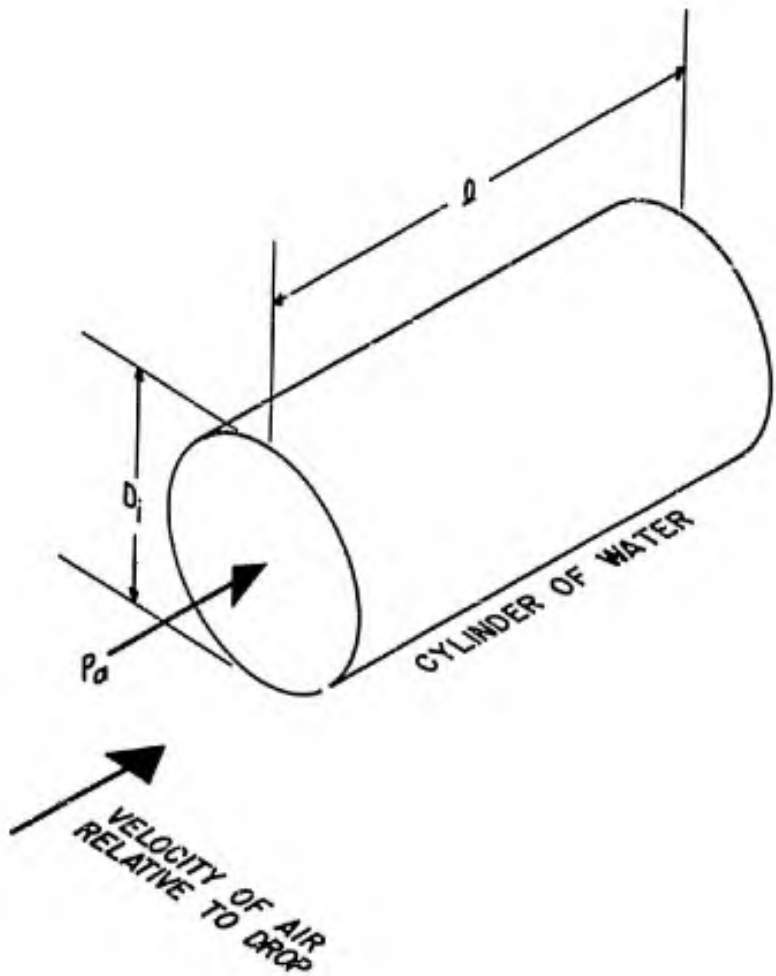

Figure 2. Drop model for Eq. (3).

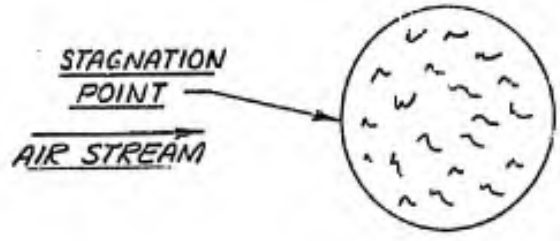

(a) INITIAL DROP CROSS SECTION

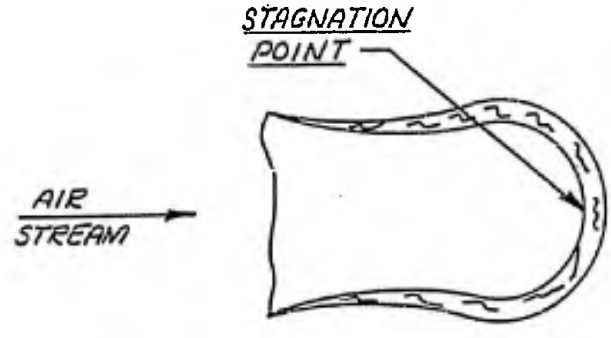

(b) DROP CROSS SECTION AFTER BEING BLOWN UP

Figure 3. Drop cross section during "Blowing-Out" type of breakup.

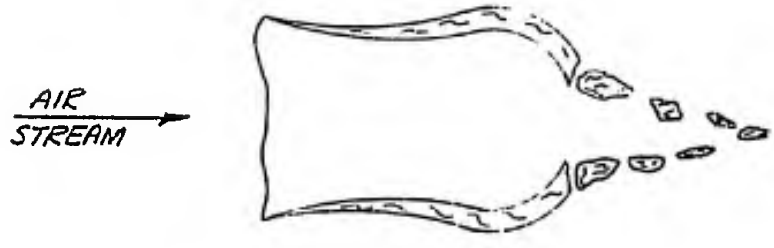

Figure 4. Drop cross section during shattering with "Blowing-Out" type of breakup.

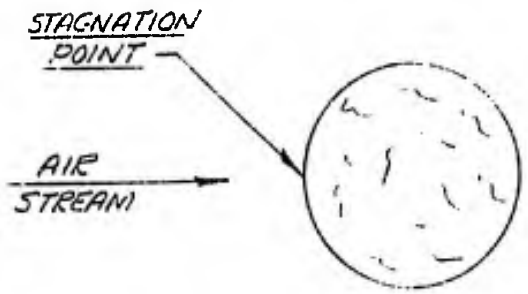

(a) INITIAL DROP CROSS SECTION

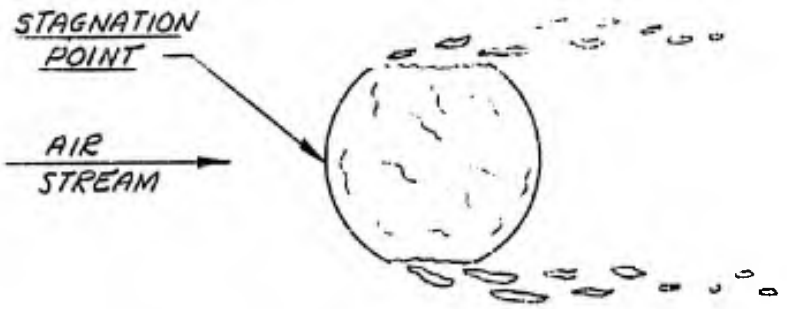

(b) DROP CROSS SECTION DURING STRIPPING ACTION

Figure 5. Drop cross section during "Stripping" type of breakup.

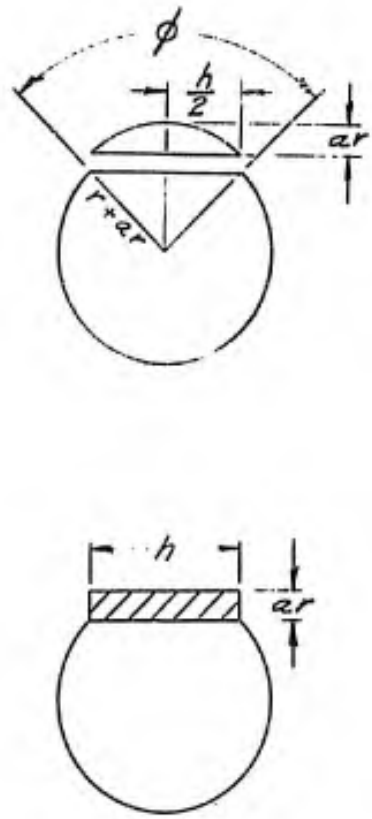

Figure 6. Drop geometry for "Stripping" type of breakup.

Symbol	Explanation
$v_o = 0$	free stream air velocity
v_m	missile velocity
v_{d_o}	drop velocity before shock
v_{d_1}	drop velocity between shock and trapped-air region
v_{d_2}	drop velocity in trapped-air region ($v_{d_o} \cong v_{d_1} \cong v_{d_2} \cong 0$)
v_2	velocity of air in separated boundary layer ($v_2 \cong v_m$)

NOTE: All velocities are with respect to the free stream.

Figure 7. Raindrop breakup in a separated flow regime.

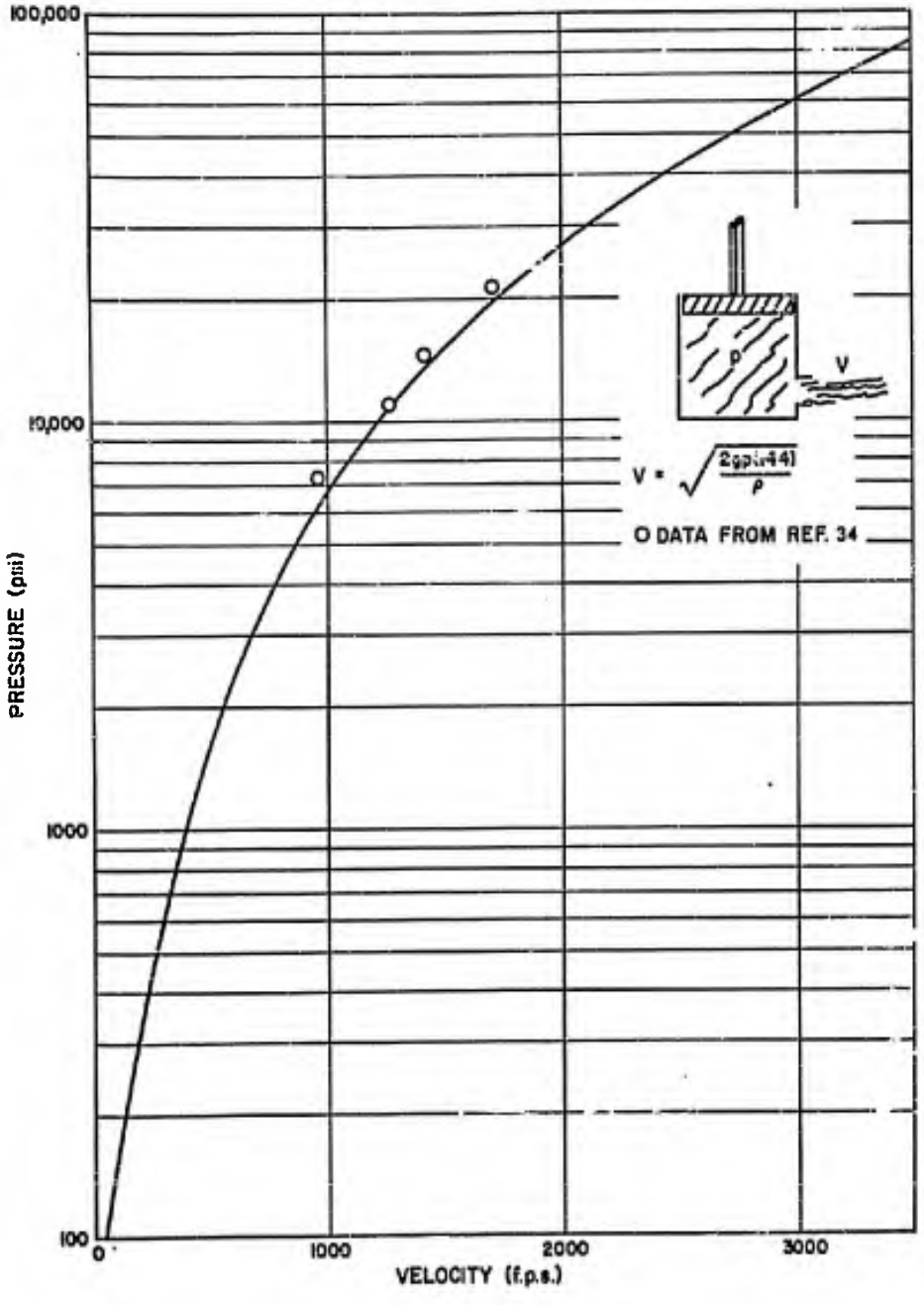

Figure 8. p versus jet velocity.

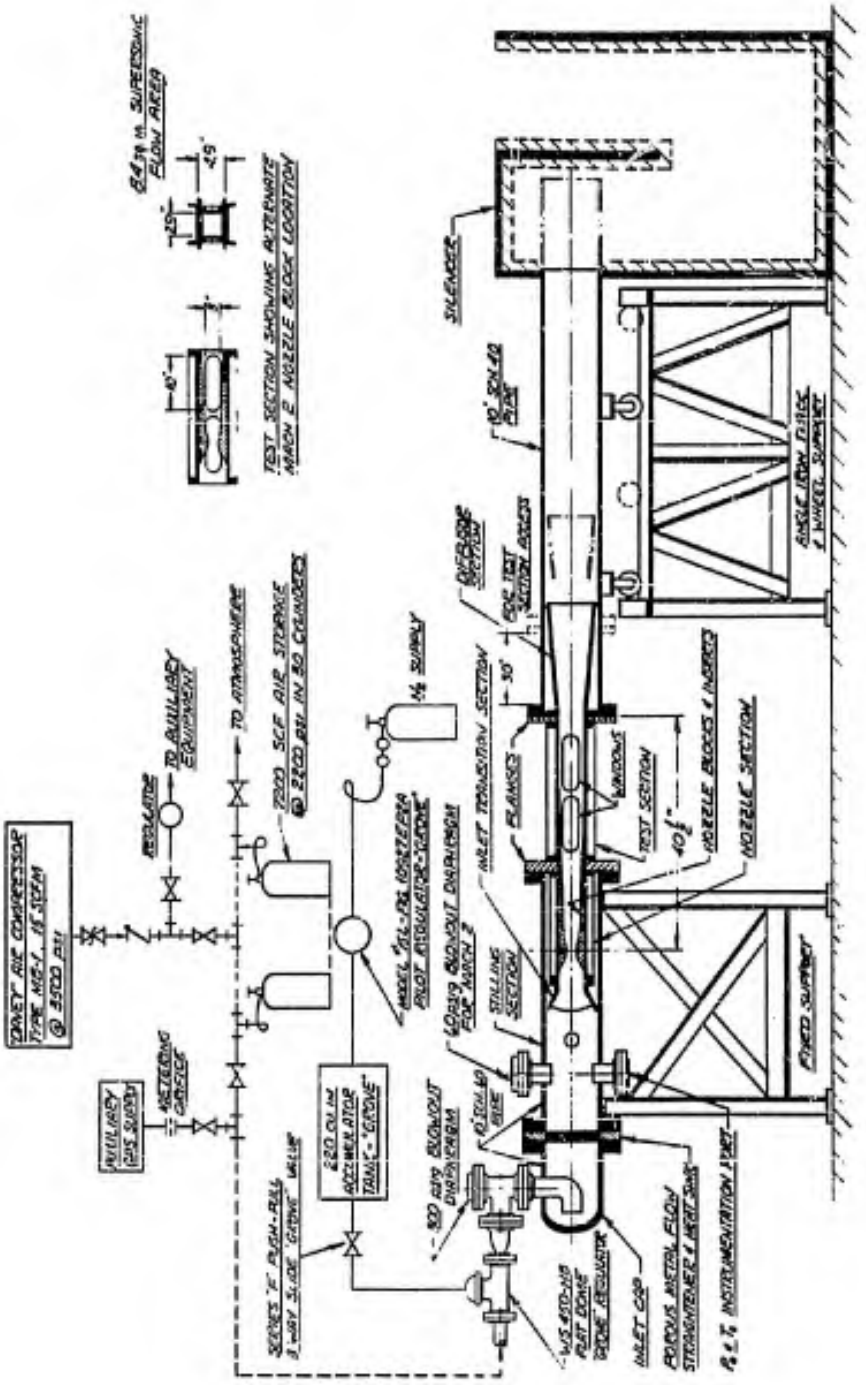

Figure 9. Schematic drawing of erosion simulator.

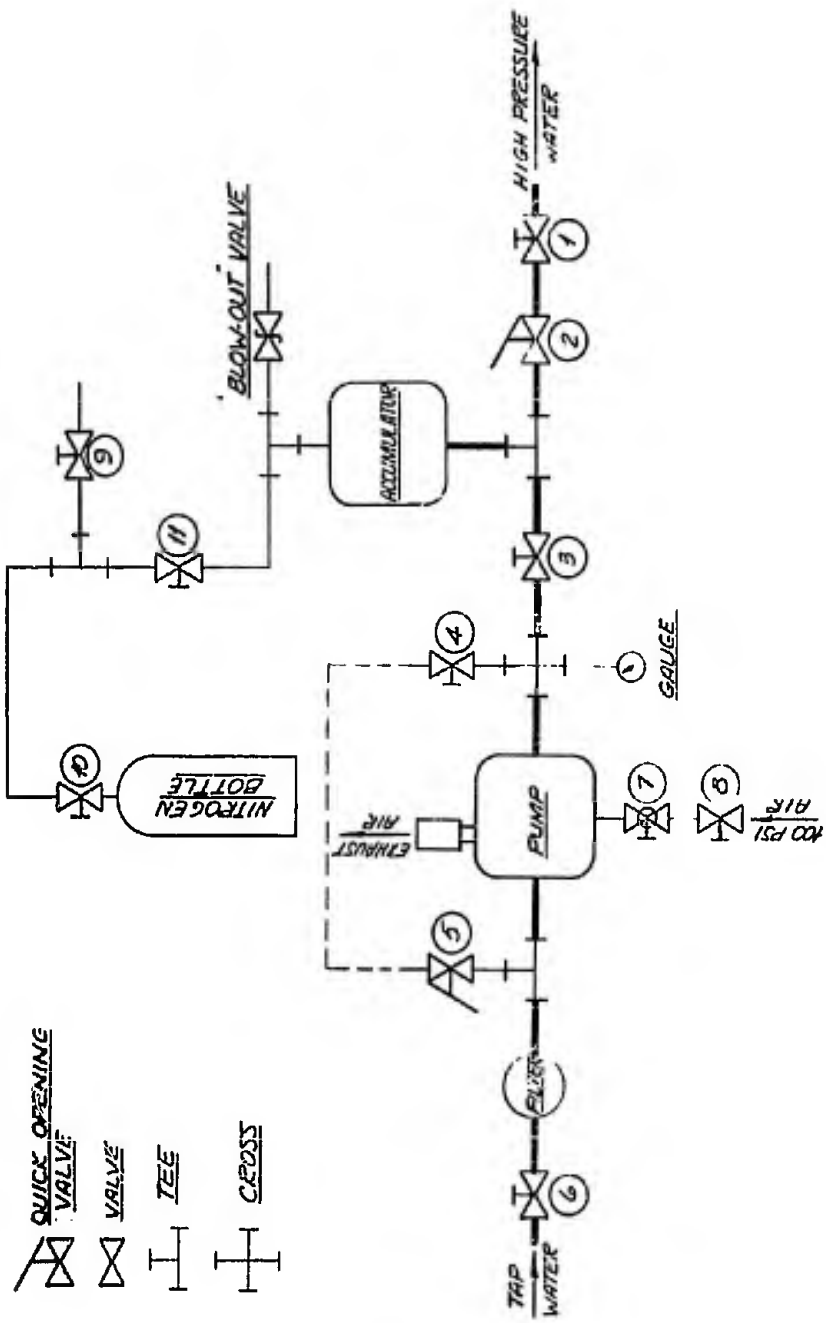

Figure 16. Schematic diagram of water pumping system.

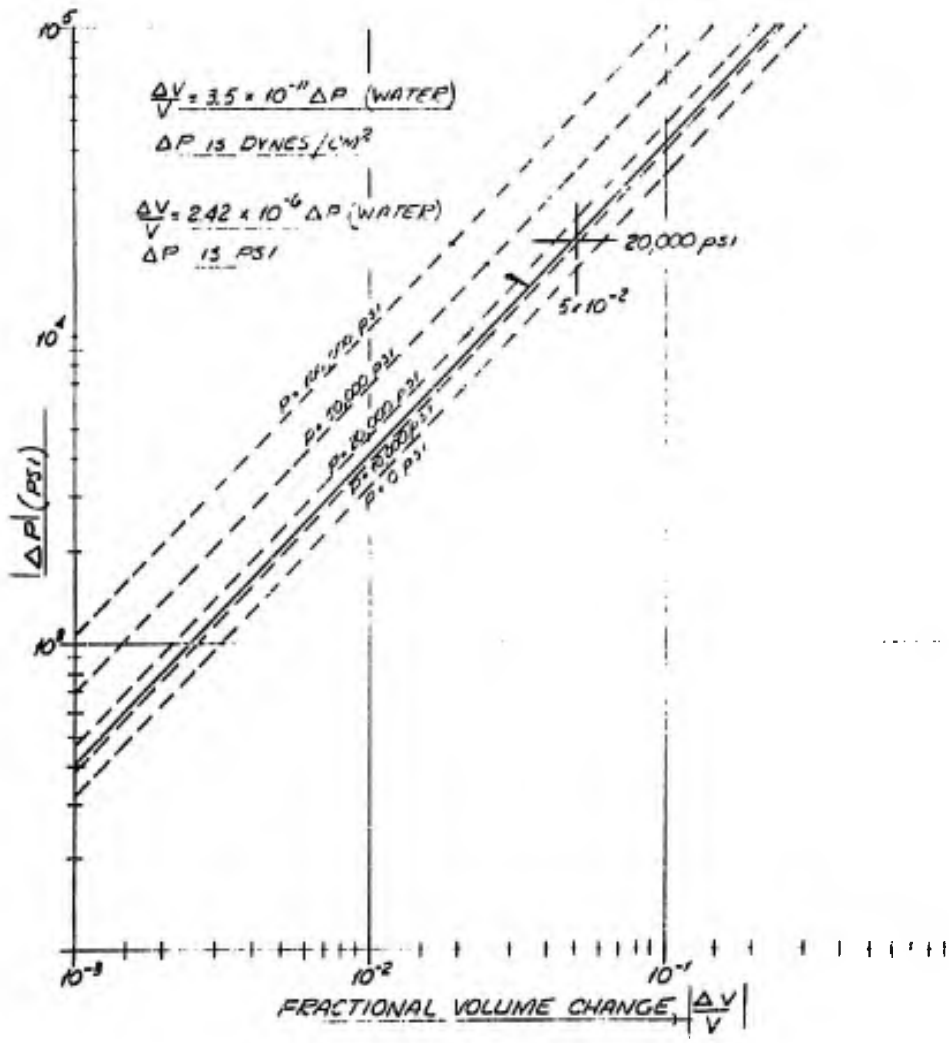

Figure 11. Pressure drop versus volume change for water-filled accumulator

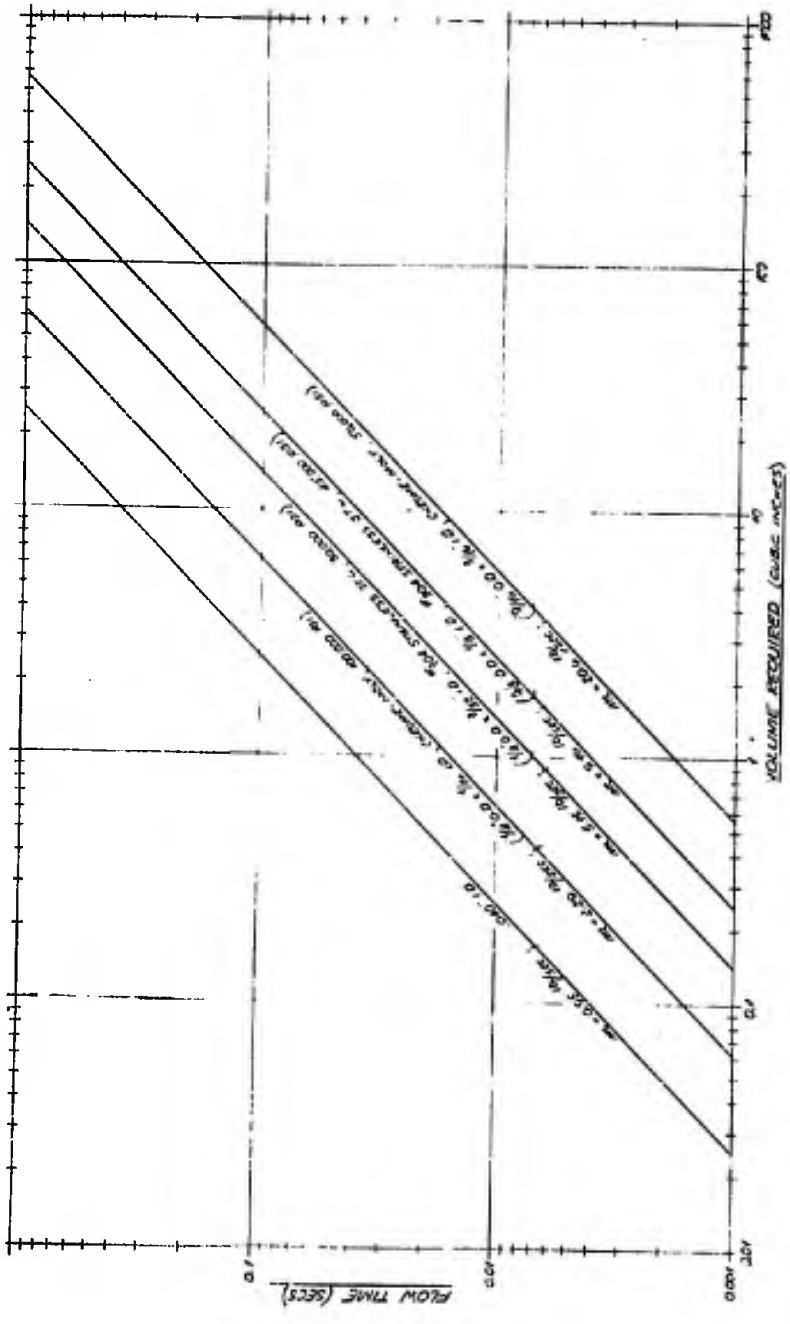

Figure 12. Flow time versus water volume required.
v = 1682 ft/sec.

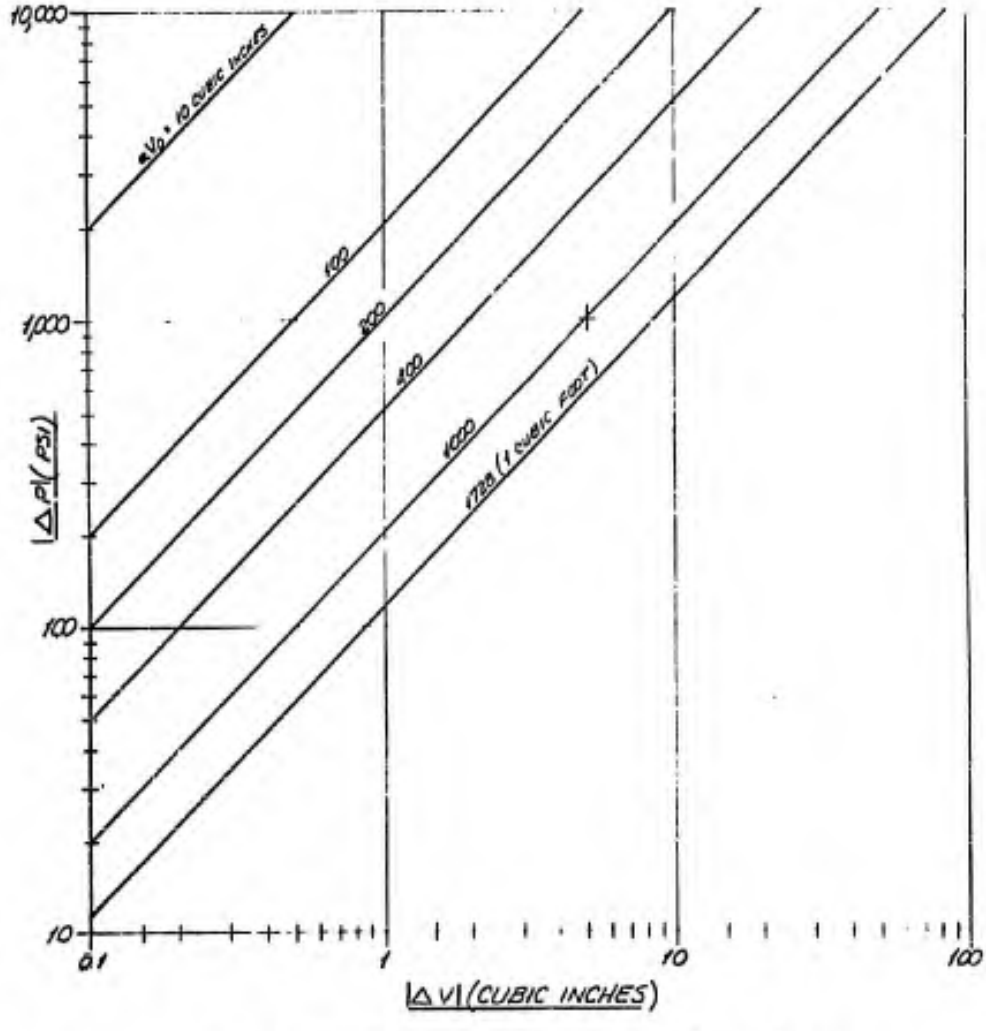

Figure 13. Pressure drop versus volume change for nitrogen charged accumulator.

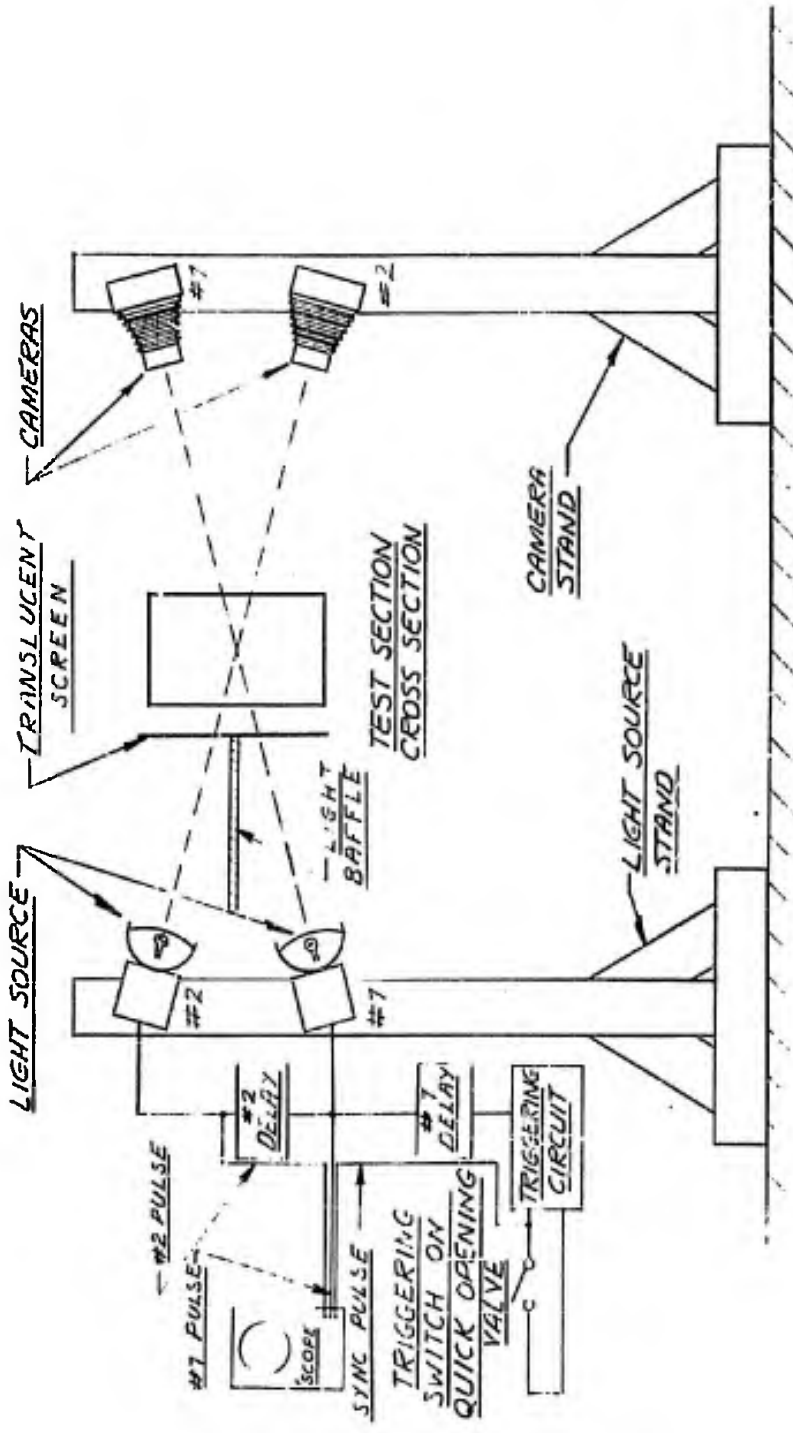

Figure 14. Photographic equipment arrangement.

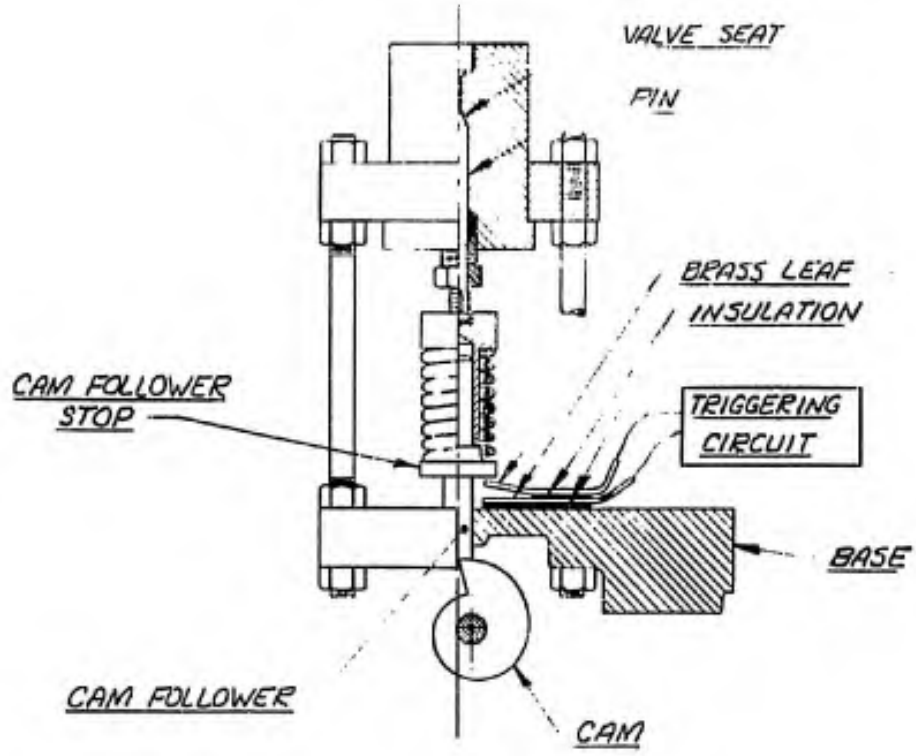

Figure 15. Electronic triggering switch on quick opening valve.

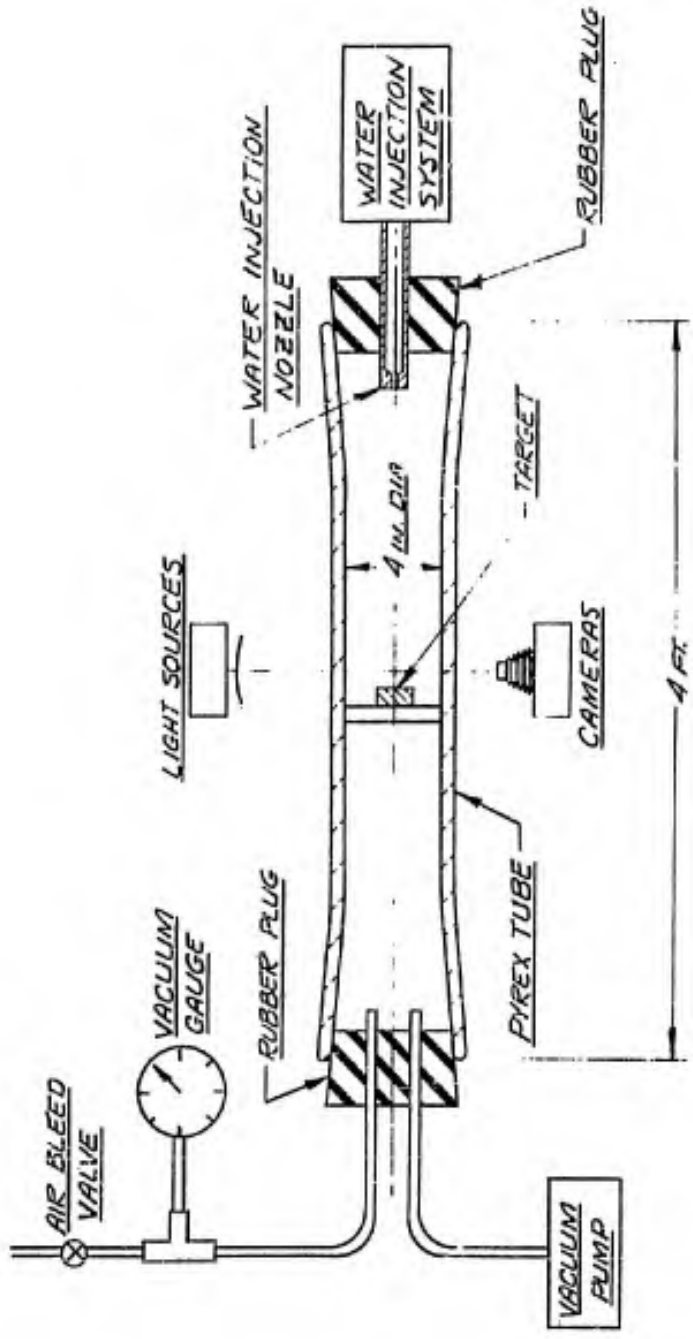

Figure 16. Equipment used in checkout of hydraulic and photographic systems.

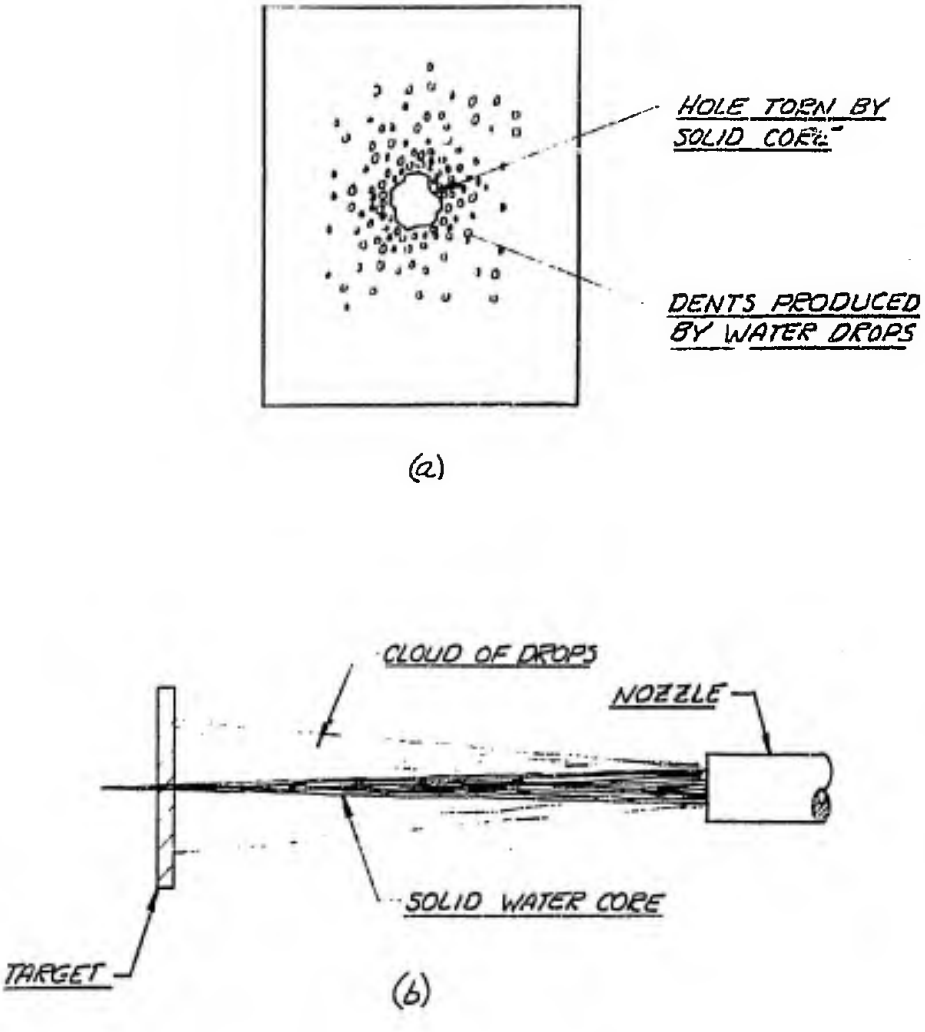

Figure 17. Jet cross section.

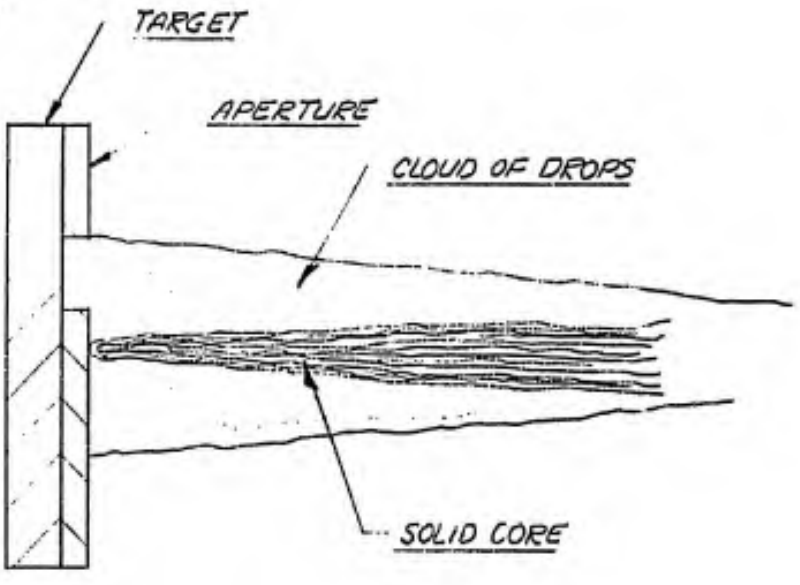

Figure 18. Target-aperture jet geometry.

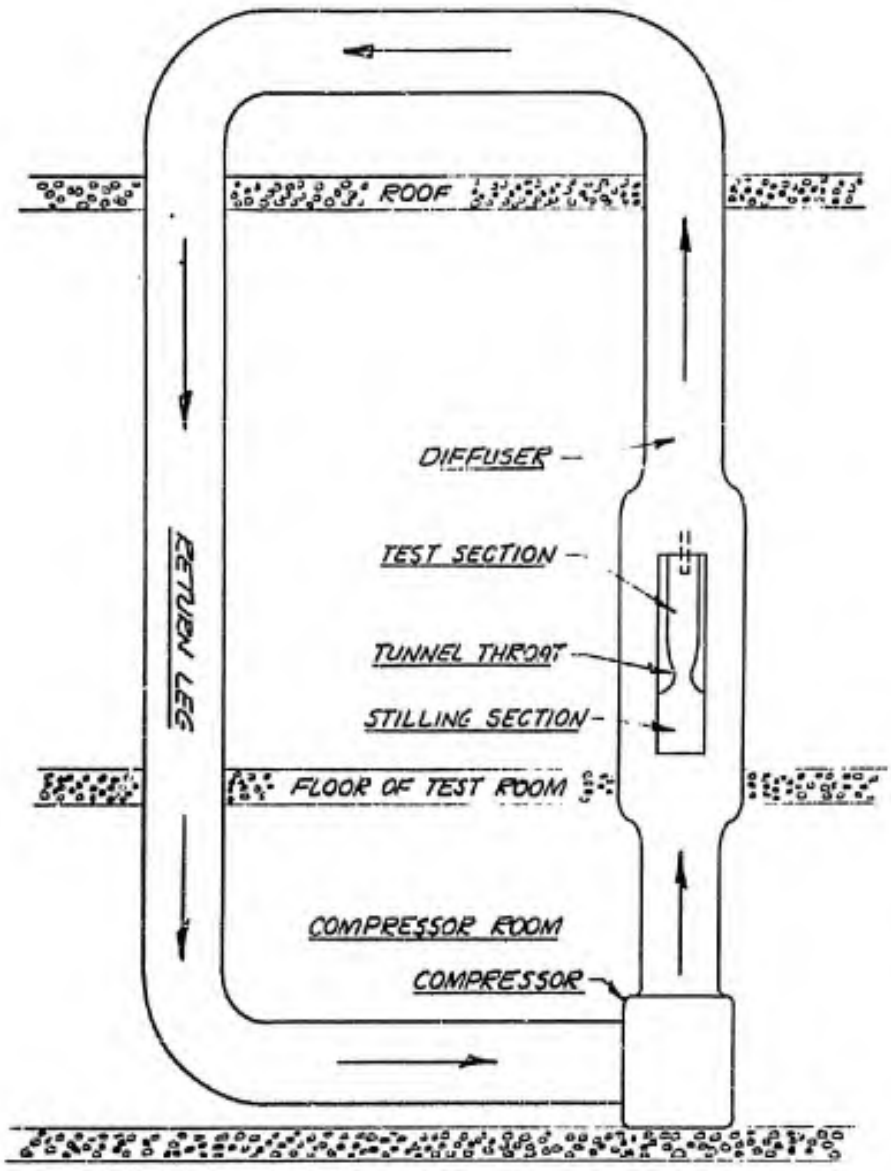

Figure 19. Tunnel circuit of Gas Turbine Laboratory.

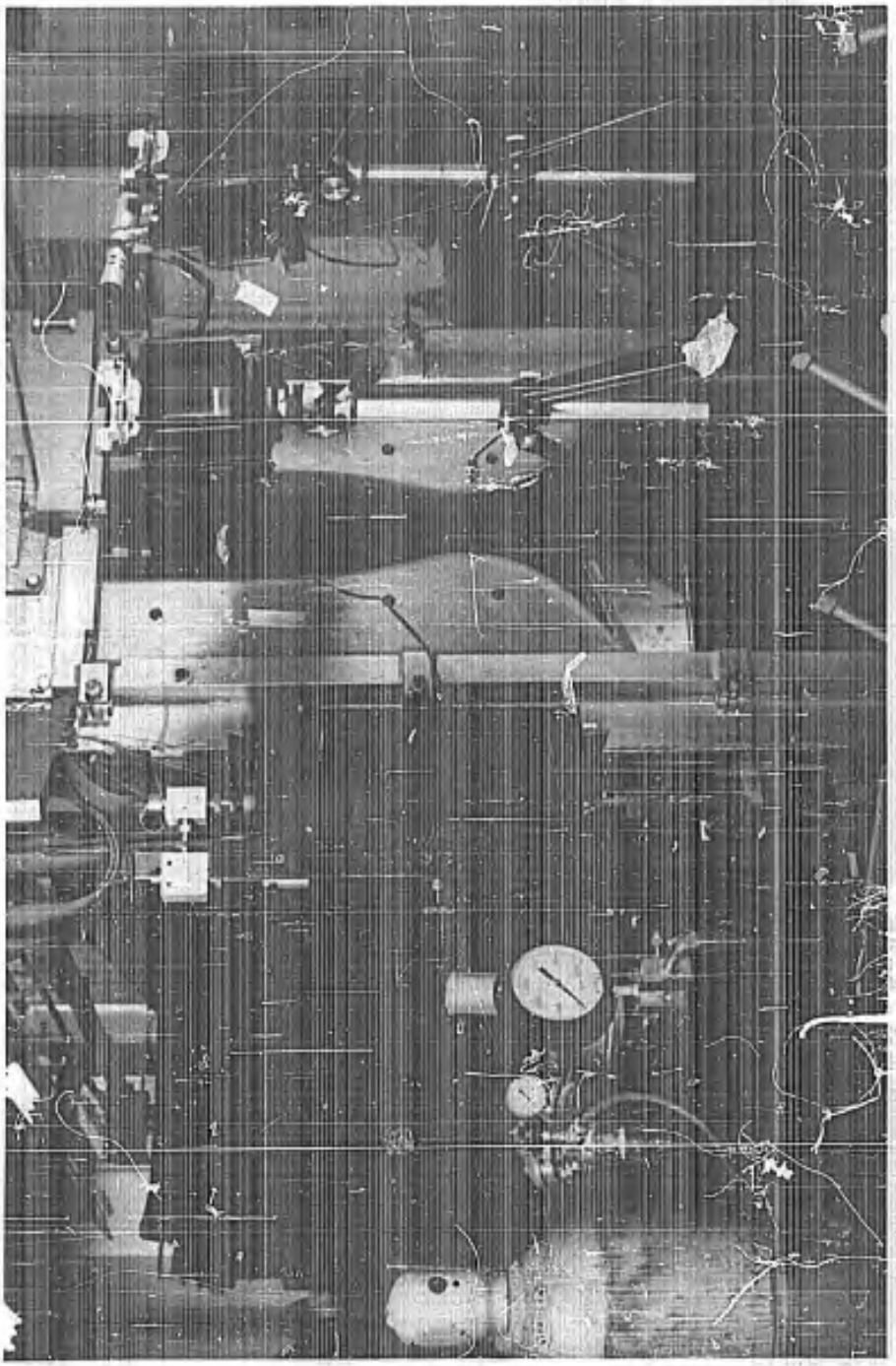

Figure 20. View of Gas Turbine Laboratory tunnel with photographic system in position and doors closed.

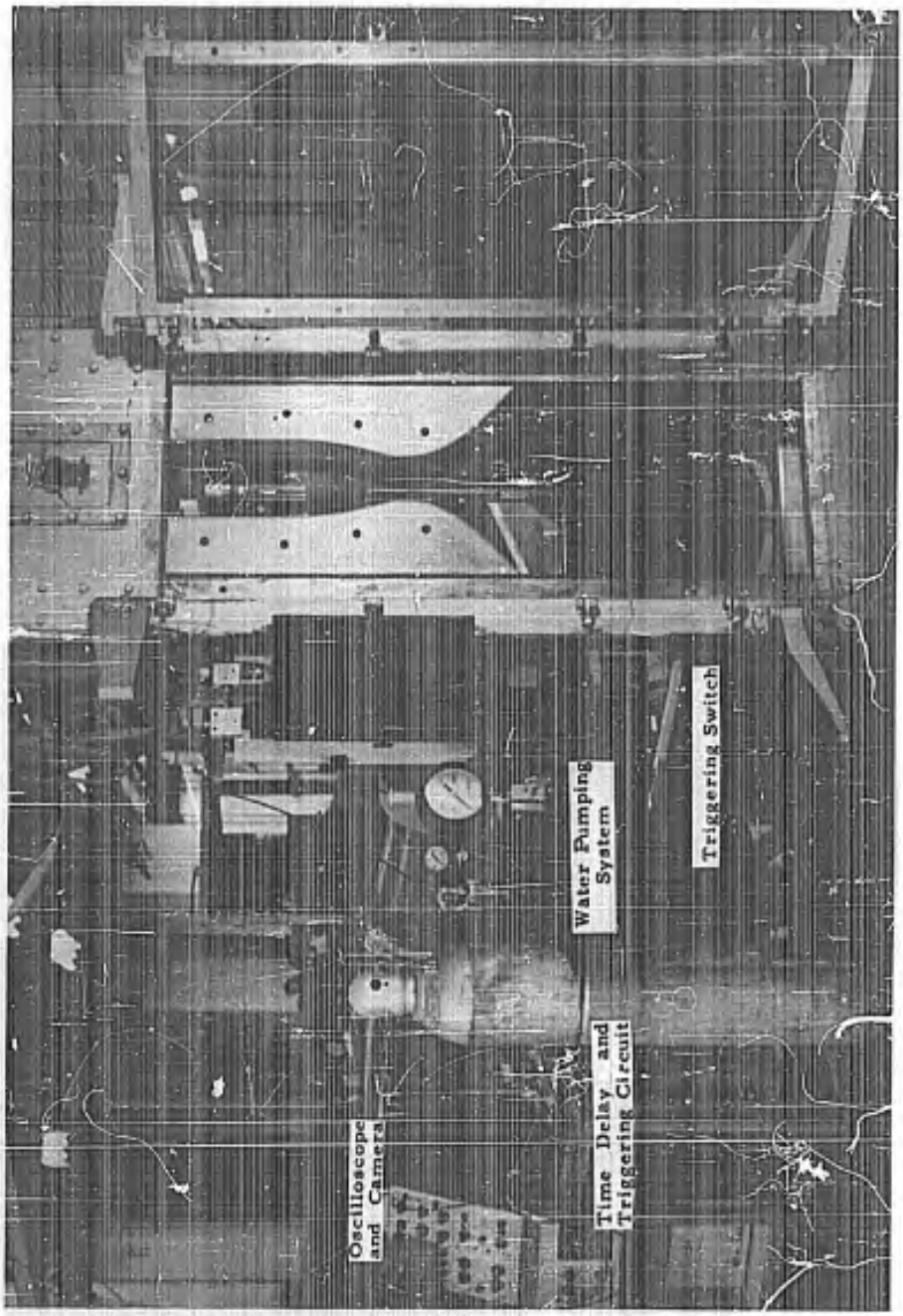

Figure 21. View of Gas Turbine Laboratory tunnel and test equipment.

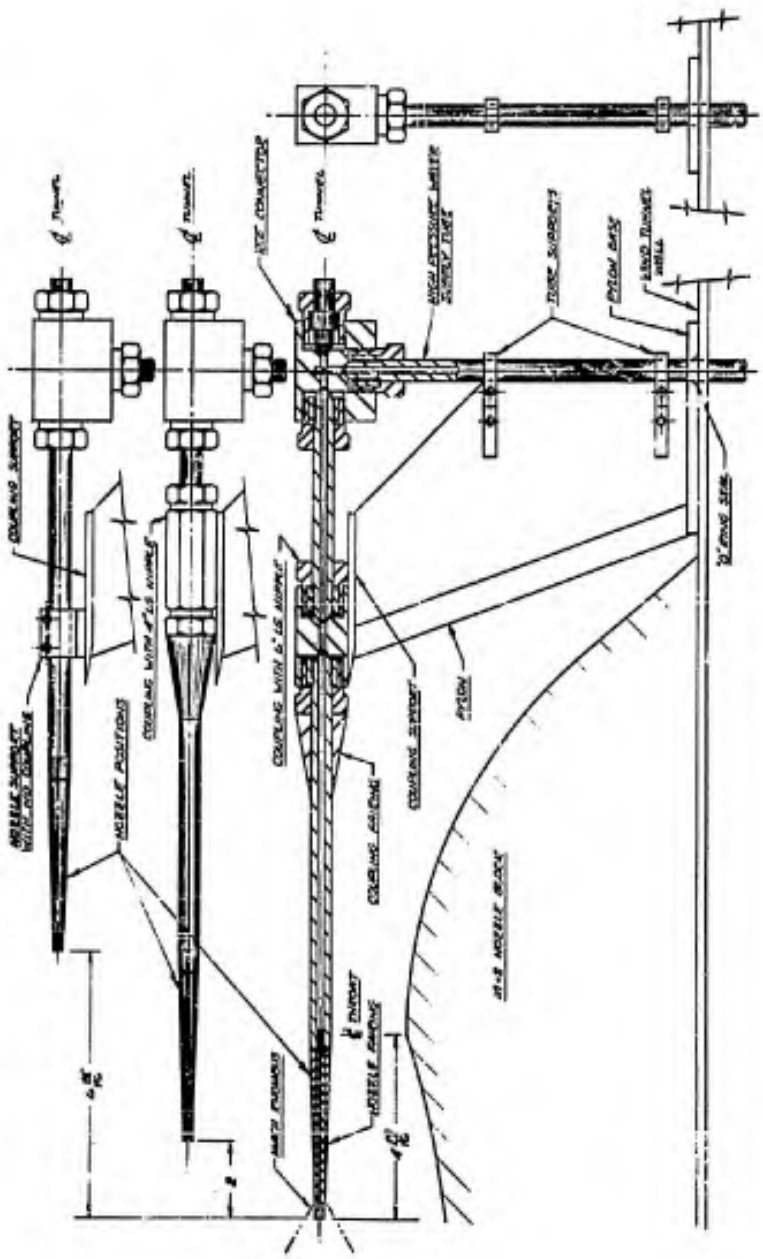

Figure 22. Water injection nozzles and support configuration.

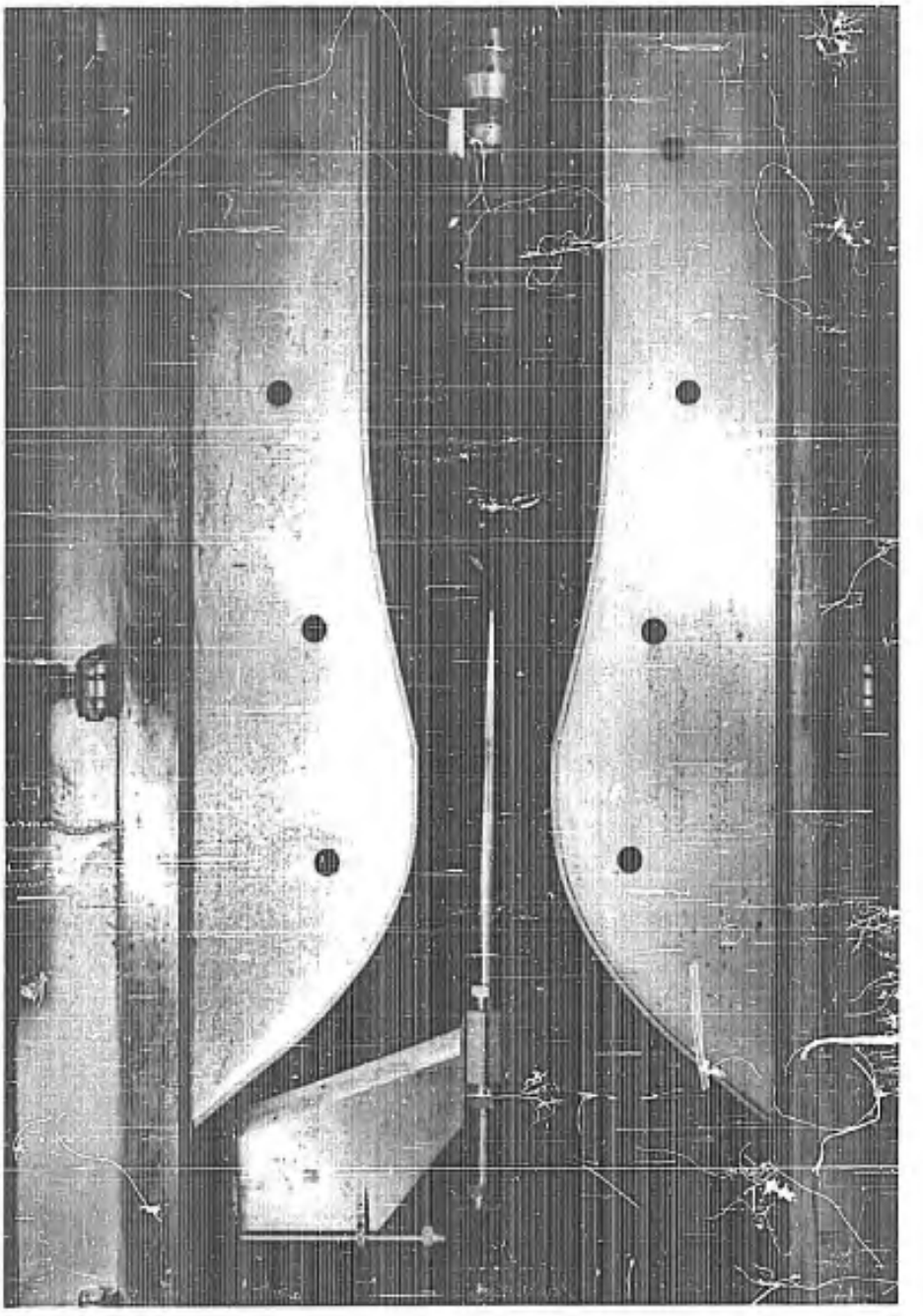

Figure 23. View of model, with sleeve, in extreme downstream position and water nozzle in extreme downstream position.

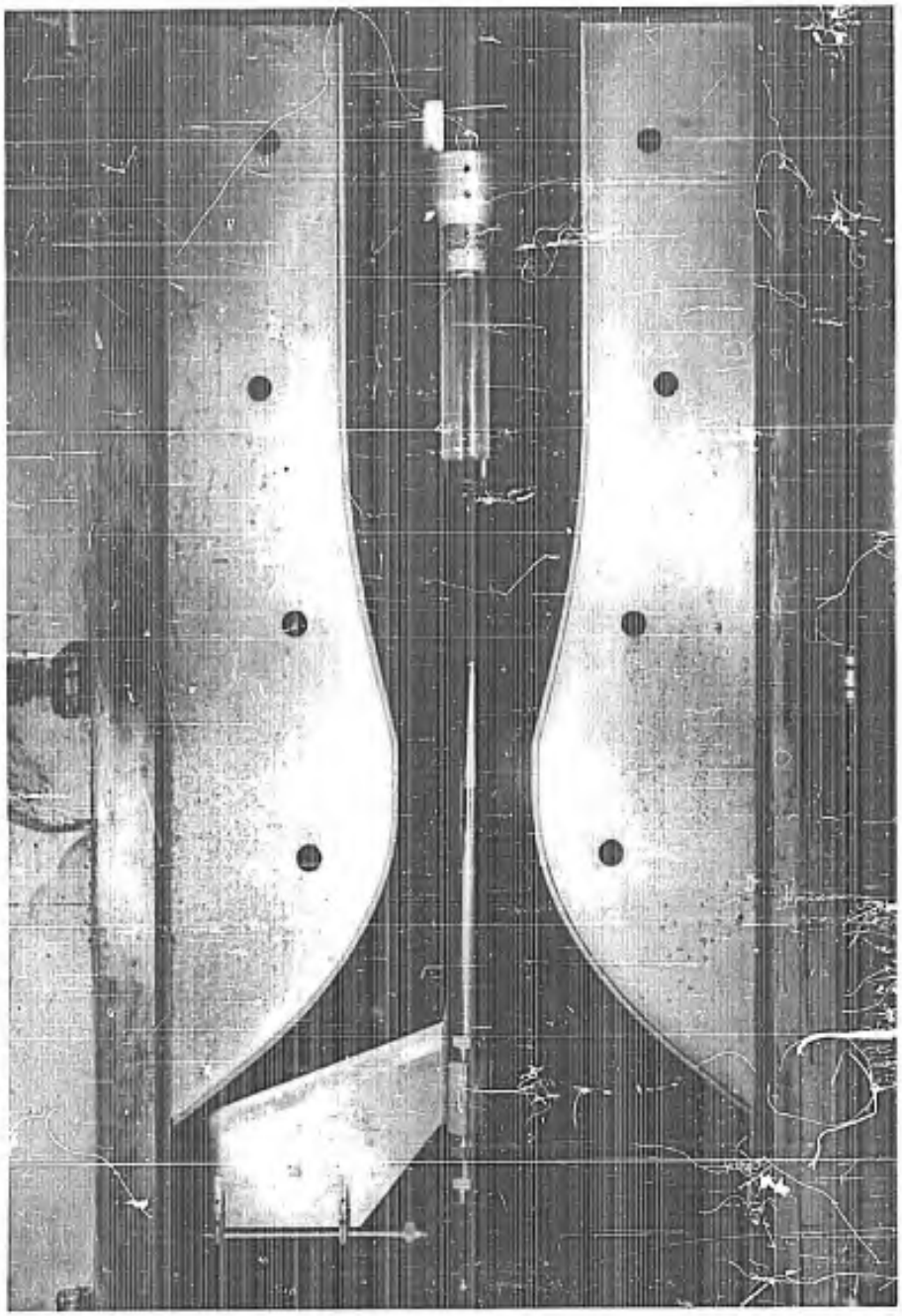

Figure 24. View of model, with sleeve, in extreme upstream position and water nozzle in mid-position.

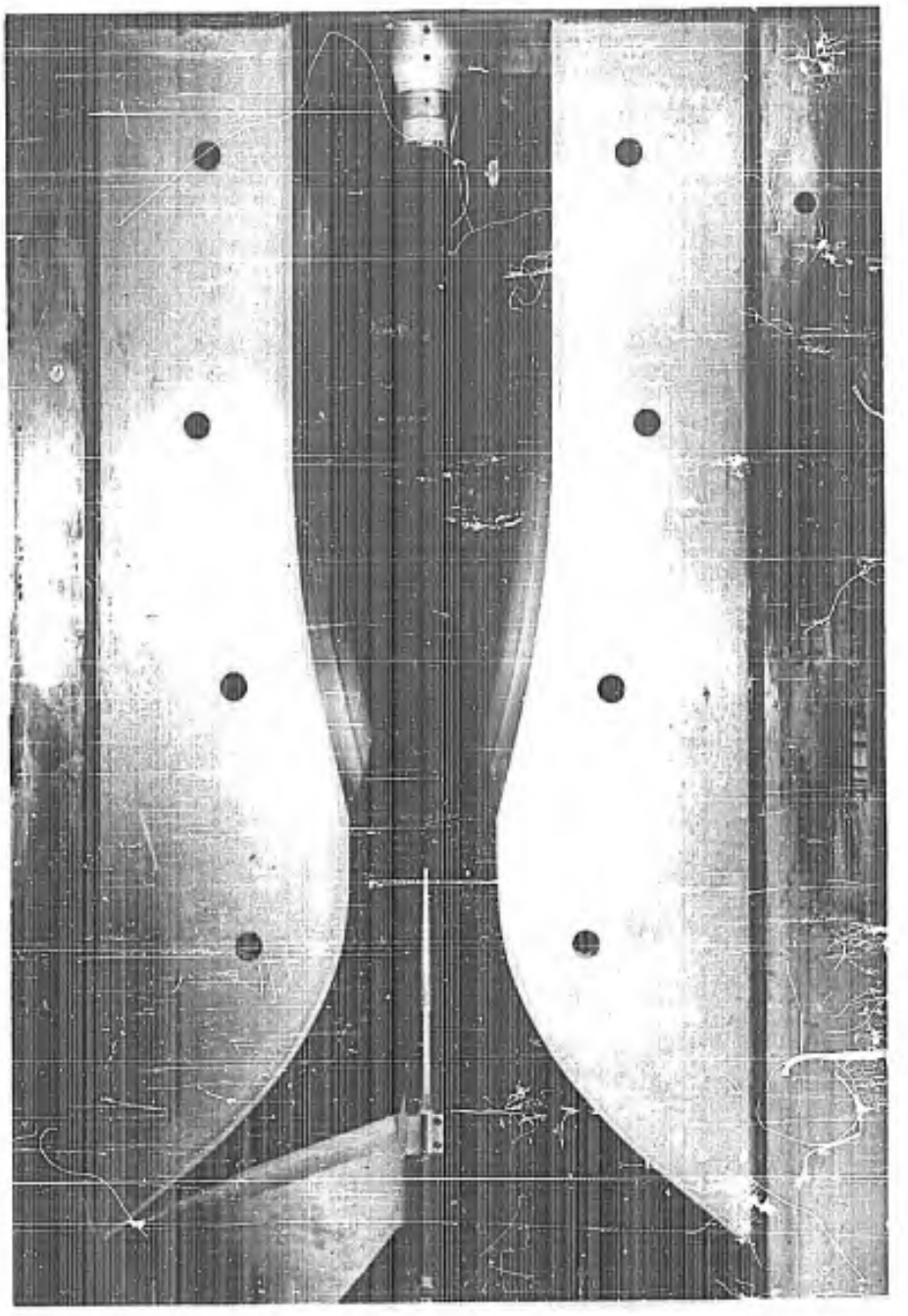

Figure 25. View of model, without sleeve, in extreme downstream position and water nozzle in extreme upstream position.

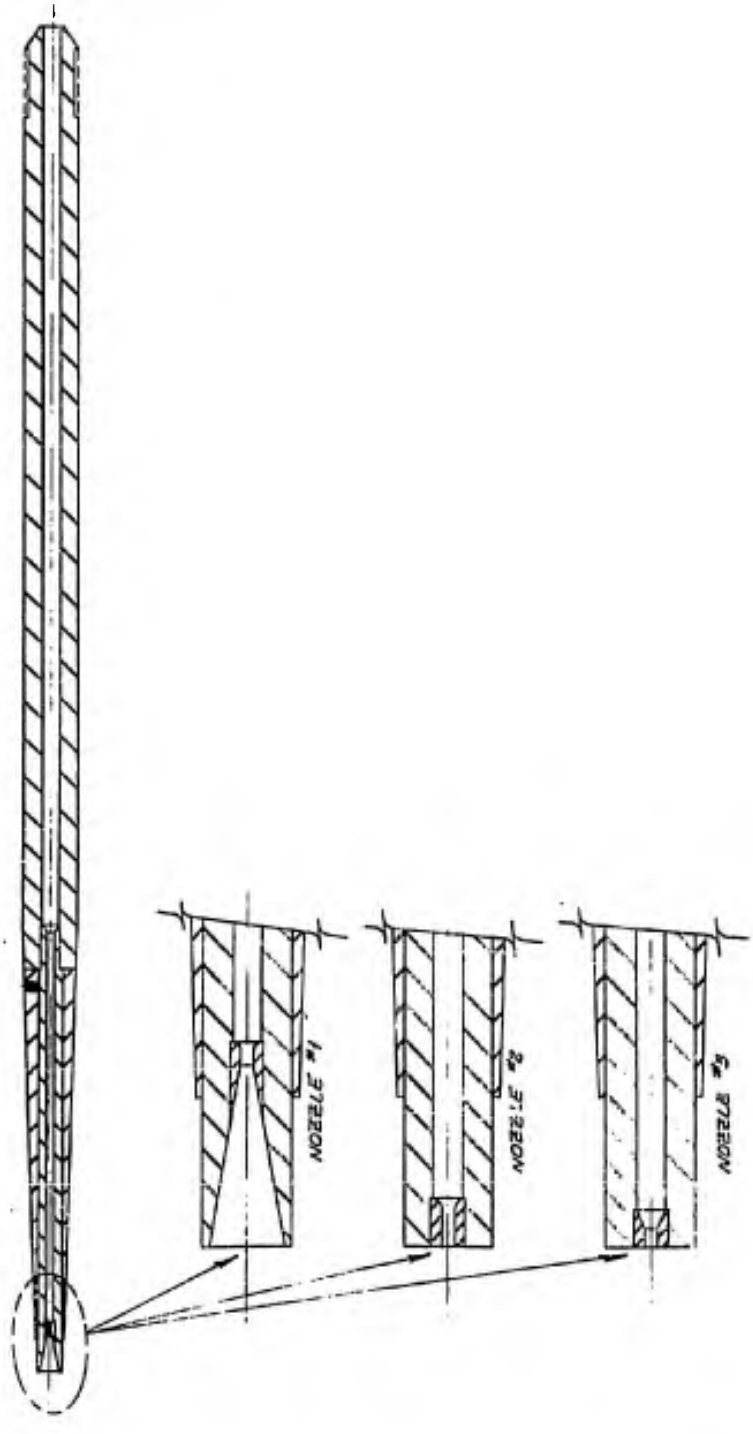

Figure 26. Water injection nozzles.

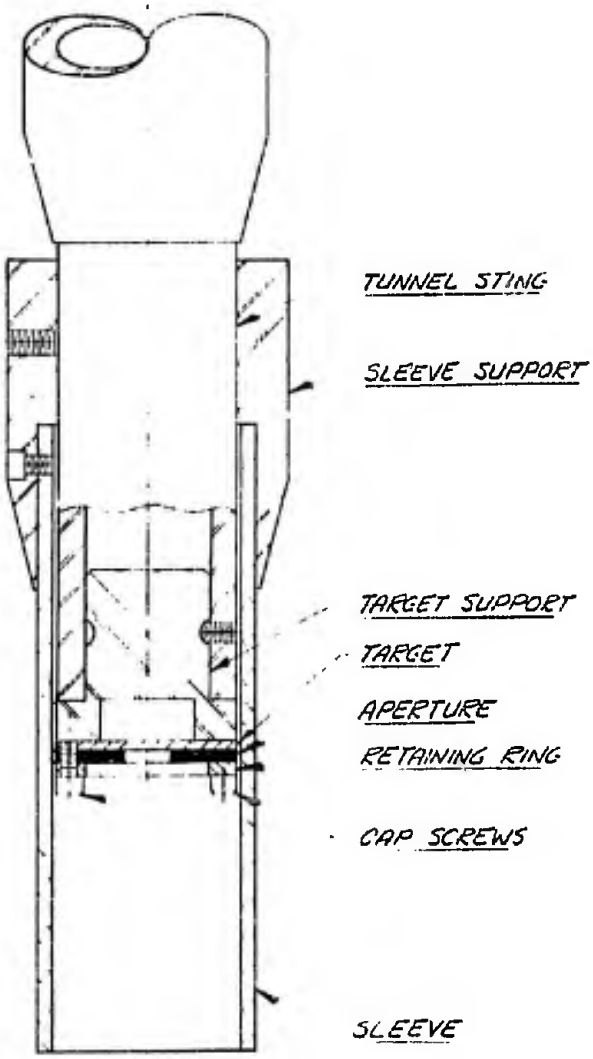

Figure 27. Model used at Gas Turbine Laboratory.

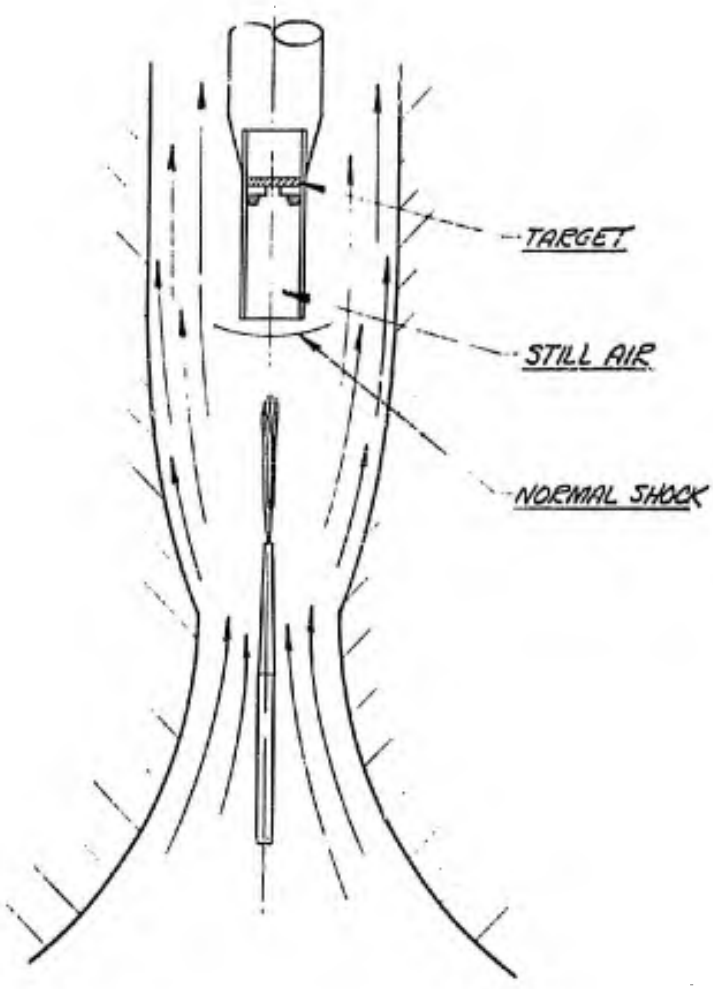

Figure 28. Model configuration in the Gas Turbine Laboratory.

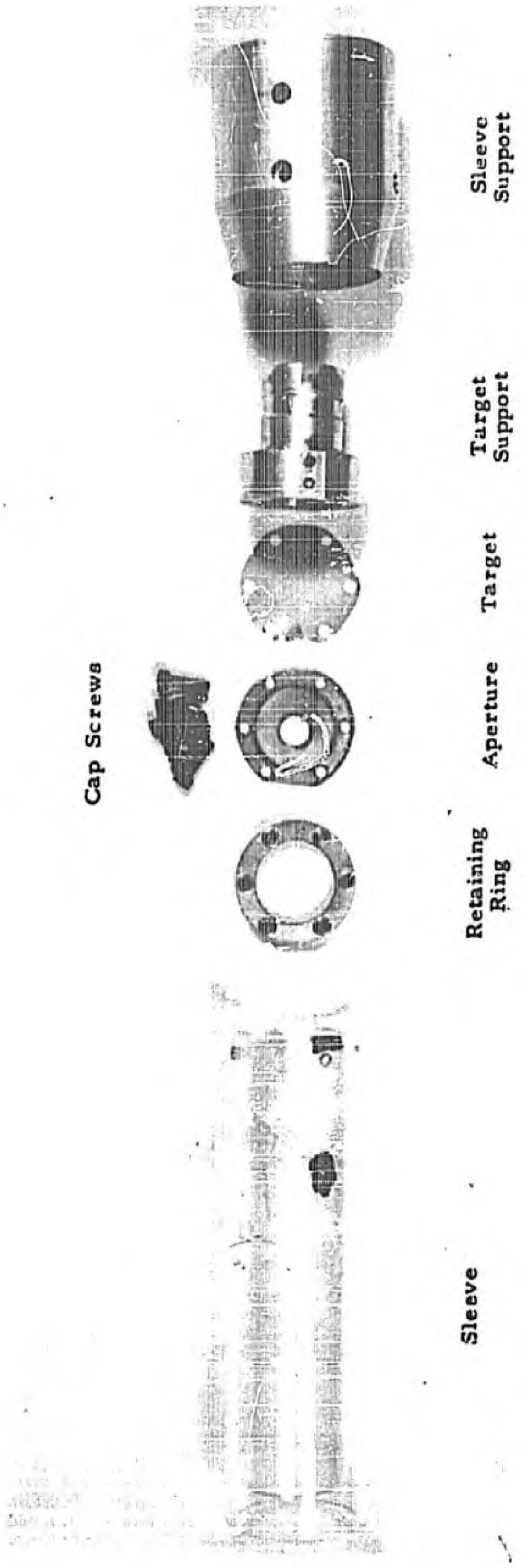

Figure 29. Exploded view of the Gas Turbine Laboratory model.

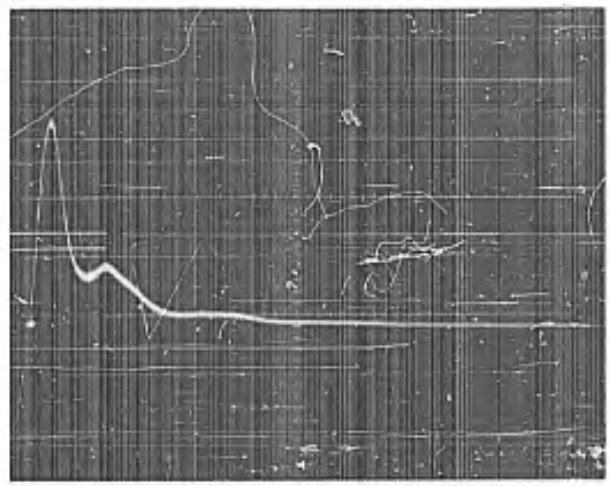

Scale: 5 μs per large division

(a) time history of light pulse

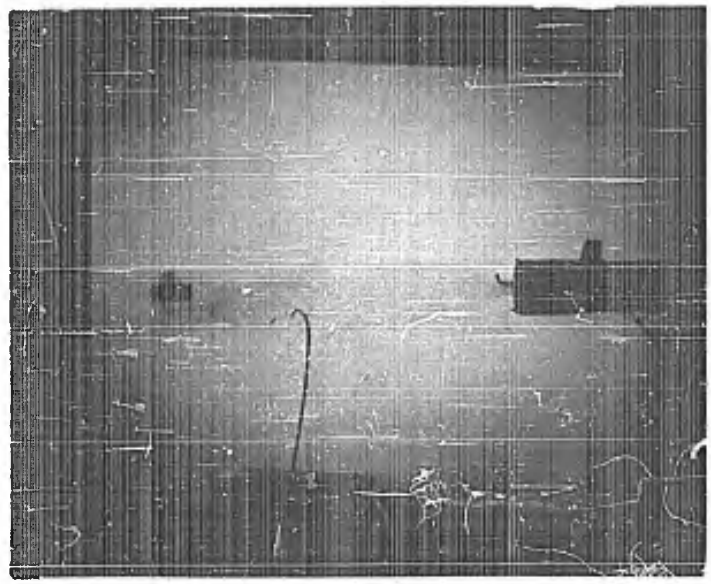

(b) photograph of 22-cal. bullet traveling at 1145 ft/sec showing blurring of image

Figure 30. Calibration of flash duration.

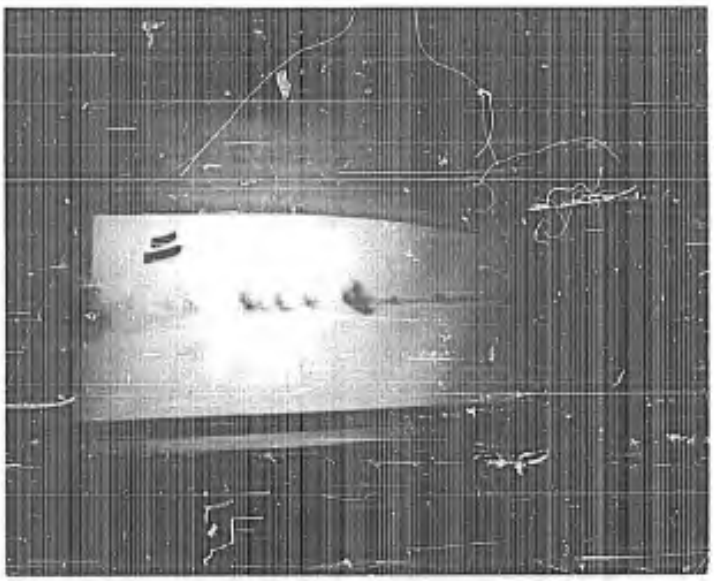

(b) second photograph

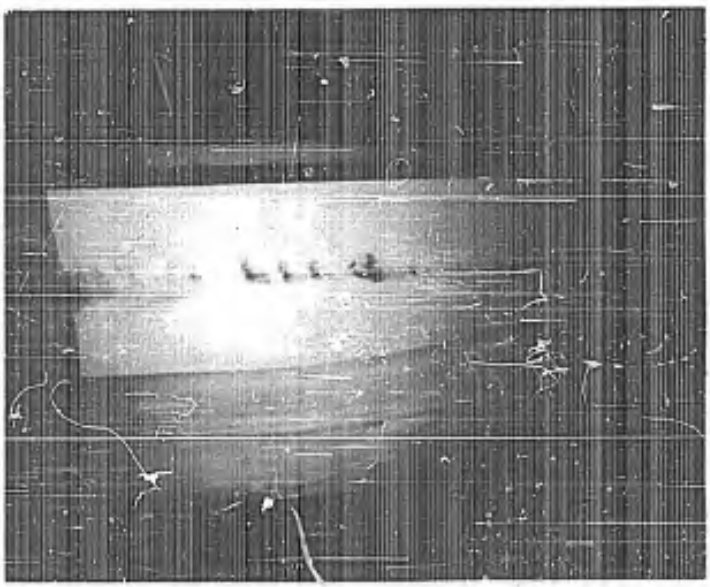

(a) first photograph

Figure 31. Run 31: Photographs of ejected water.

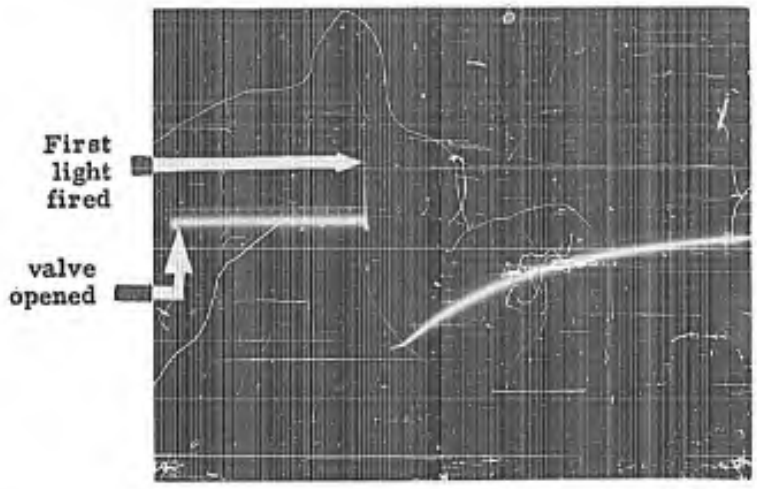

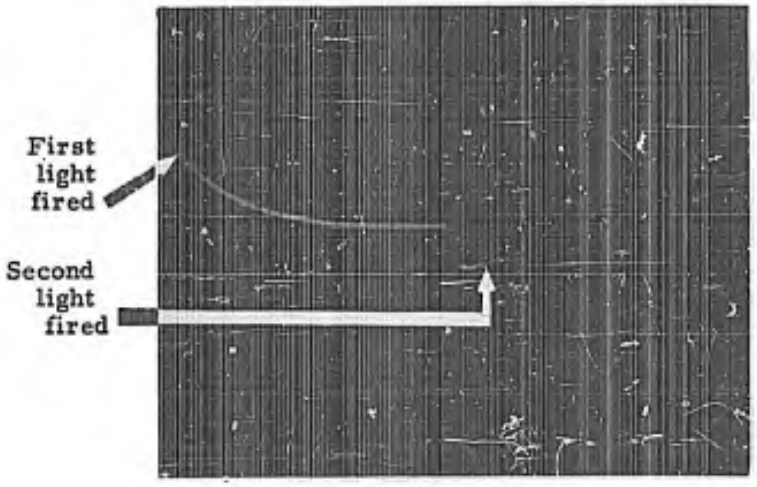

(b) time between first and second photographs

Figure 32. Run 31: Timing Marks.

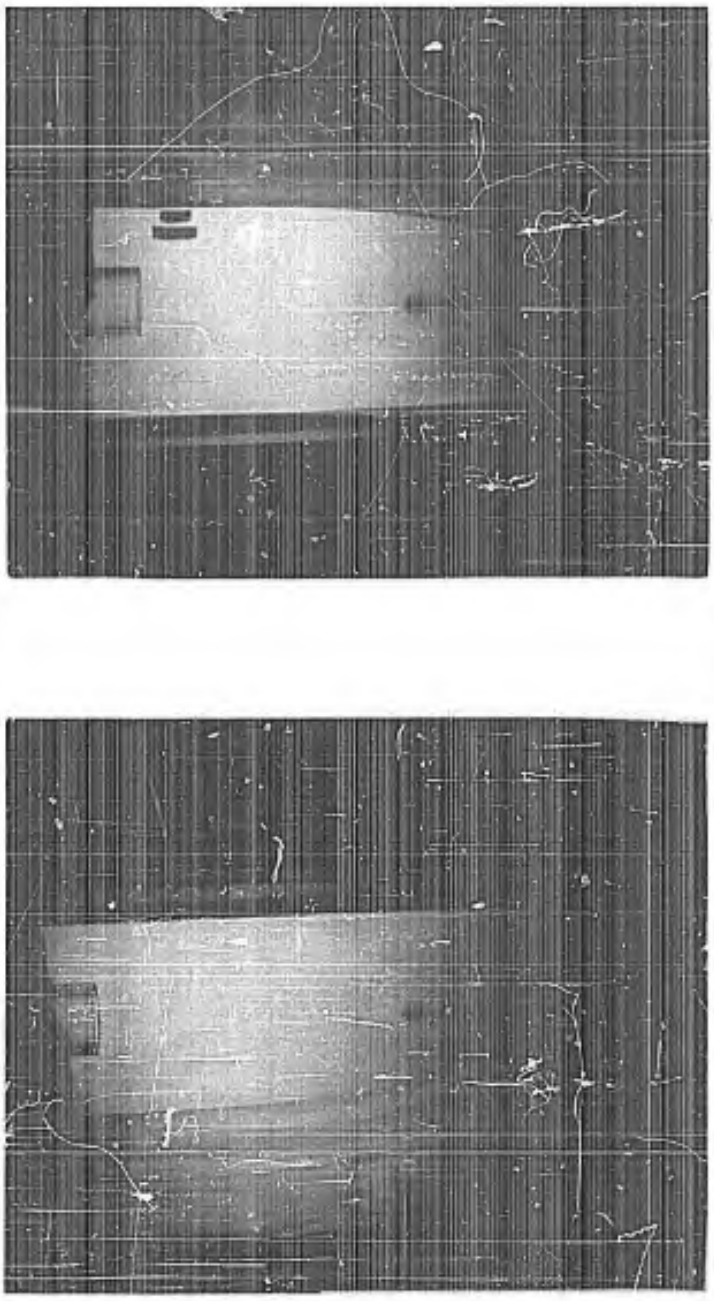

(a) first photograph

(b) second photograph

Figure 33. Run 37: Photographs of ejected water.

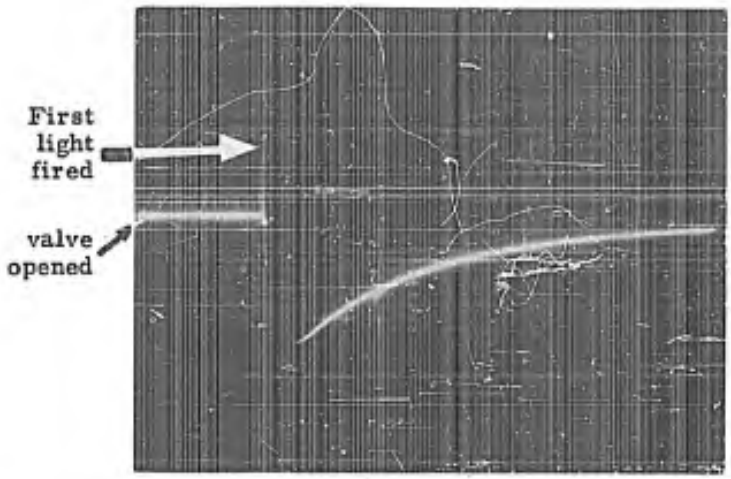

Scale: 1 ms per large division

(a) time to first photograph

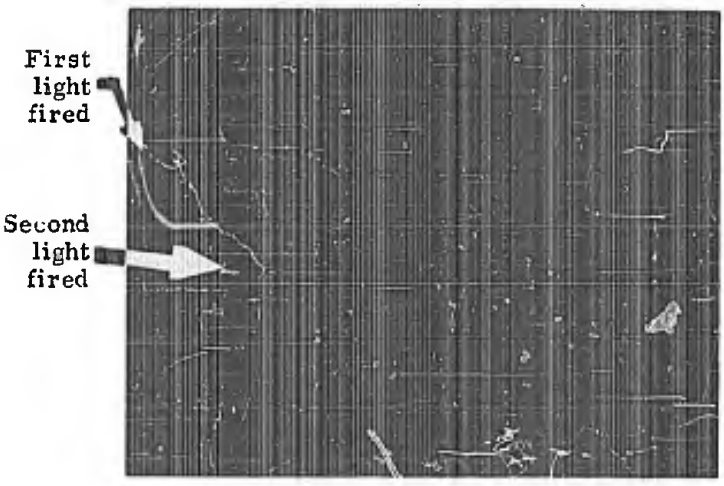

Scale: 50 μs per large division

(b) time to second photograph

Figure 34. Run 37: Timing Marks.

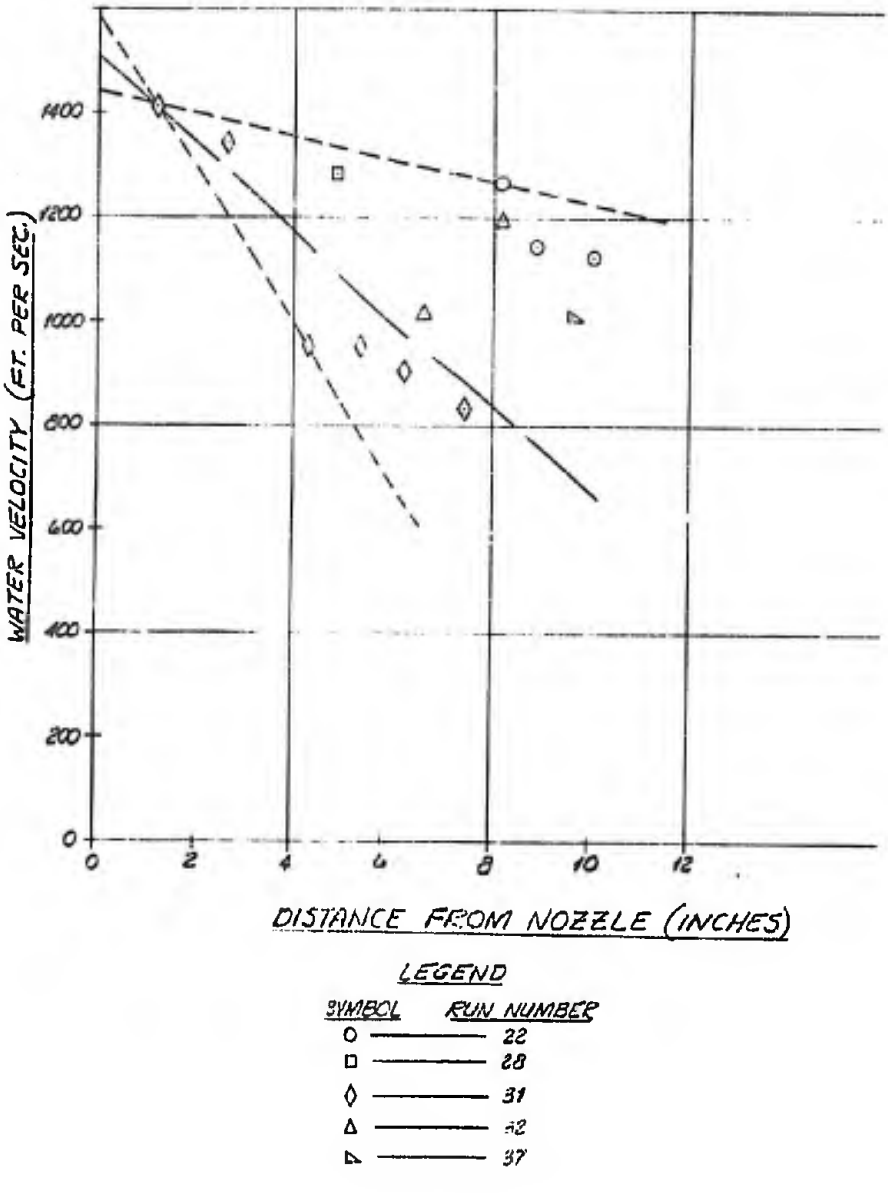

Figure 35. Water velocity versus distance from nozzle.

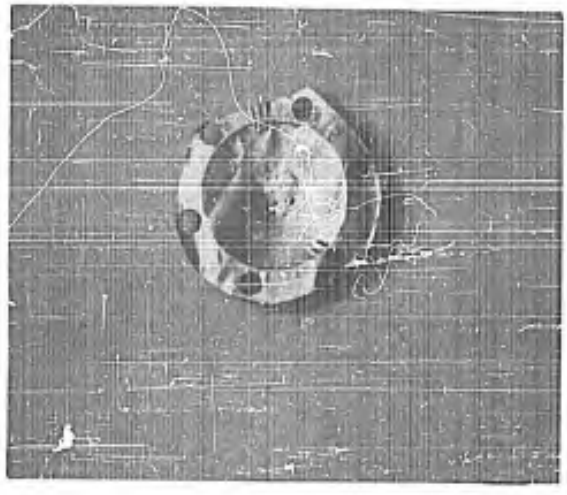

(a) Runs 22 and 23

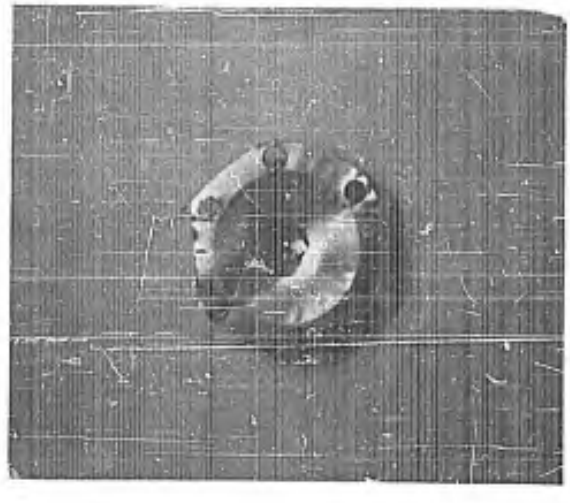

(b) Runs 35 and 36

Figure 36. Photographs of brass targets after drop impact without sleeve.

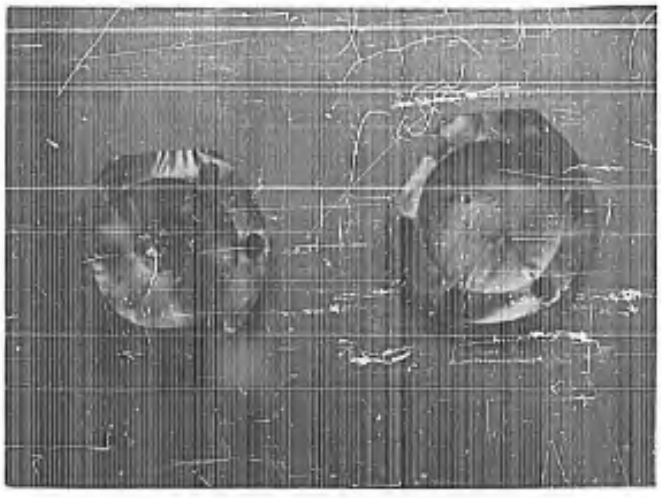

Runs 10, 11, and 12 (without sleeve)

Runs 13, 14, and 15 (with sleeve)

Figure 37. Photographs of brass targets after drop impact with and without sleeve.

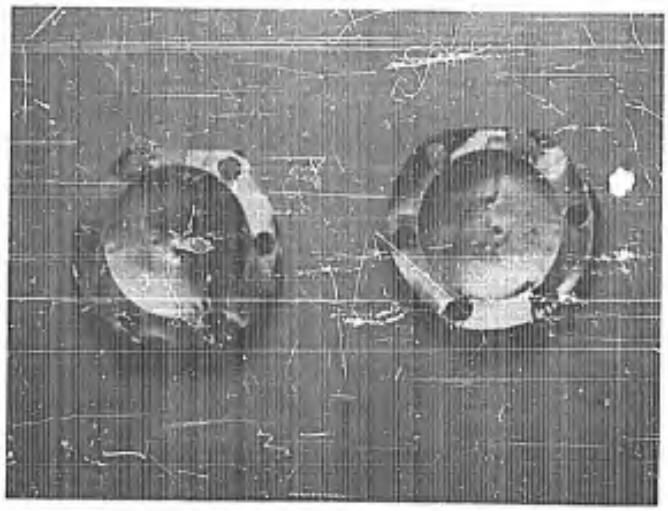

Runs, 19, 20, and 21 (without sleeve)

Runs 16, 17, and 18 (with sleeve)

Figure 38. Photographs of brass targets after drop impact with and without sleeve.

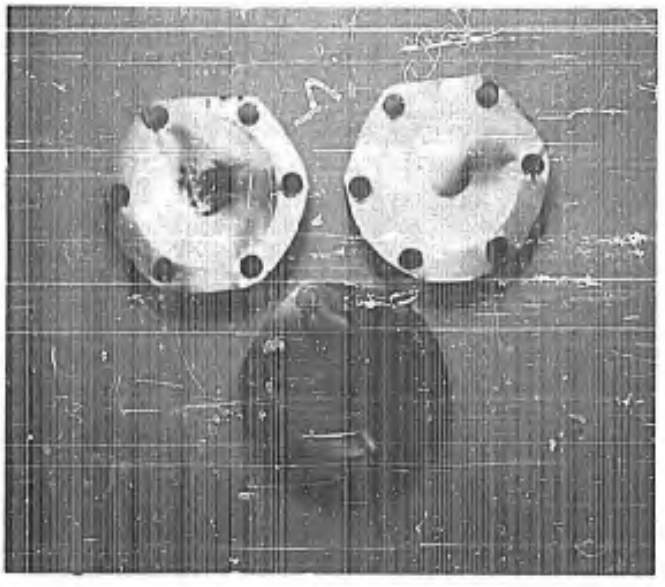

Figure 39. Photographs of brass targets after drop impact with and without sleeve and with water off.

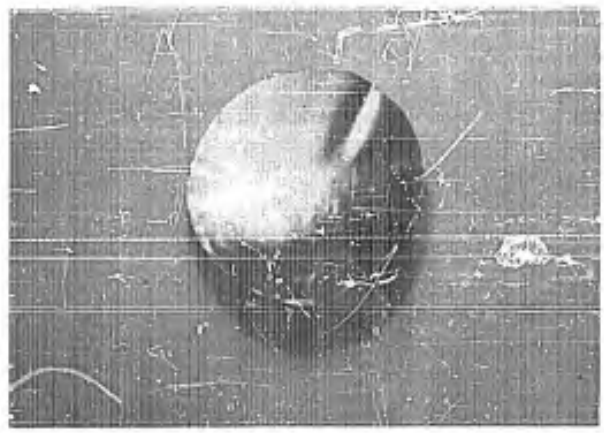

Figure 40. Photograph of brass target after drop impact during equipment checkout.

APPENDIX A

Determination of the Sleeve Length for Drop Breakup in the MIT Gas Turbine Laboratory Tunnel

The drop breakup equation (as derived by several methods) is

$$t_b \cong 0.50 \frac{D_i}{V} \left[\frac{\rho_w}{\rho_a} \right]^{1/2}$$

where

t_b = drop breakup time (seconds)

D_i = initial drop diameter (inches)

V = relative velocity between drop and gas (inches/second)

ρ_w = water drop density

ρ_a = gas density

In predicting the drop breakup distance we will take the gas conditions to be those at stagnation behind a normal shock at Mach 2. The tunnel stagnation conditions are taken as

$$p_t = 14.7 \text{ psia}$$

$$T_t = 530^\circ R$$

From Ref. 47 we have

$$p_{t_2}/p_{t_1} = 0.7209$$

$$p_{t_2} = 0.7209 \times 14.7 = 10.6 \text{ psia}$$

$$T_{t_2} = T_{t_1} = 530^\circ R$$

$$\rho_{t_2} = \frac{P_{t_2}}{R\,T_{t_2}} = \frac{10.6 \times 144}{1716 \times 530} = 0.00168 \ \frac{sl}{ft^3}$$

$$\rho_w = 62.4 \ \frac{lb}{ft^3}$$

$$\frac{\rho_w}{\rho_a} = \frac{62.4/32.2}{0.00168} = 1155$$

$$\sqrt{\rho_w/\rho_a} = 34.0$$

$$t_b = 0.5 \ \frac{D_i}{V} \ 34.0$$

We will take

$$D_i = 0.040 \text{ inches}$$

$$V = 1682 \times 12 \text{ inches/sec}$$

thus

$$t_b = \frac{0.5 \times 0.04 \times 34.0}{1682 \times 12}$$

$$t_b = 3.37 \times 10^{-5} \text{ seconds}$$

D_b = drop breakup distance

$$D_b = 0.68 \text{ inches}$$

The drop breakup equation, as used here, has a coefficient of 0.50. This constant has been reported to be as high as 2.0 so that the drop breakup distance should lie in the range

$$2.72 \text{ inches} > D_b > 0.68 \text{ inches}$$

Therefore a sleeve length of 3 inches or more should be sufficient to break up all drops.

APPENDIX B

Pressure Losses in Water Injection System

The pressure losses in smooth straight pipes with turbulent flow is given in Ref. 37 by

$$\Delta p = \left(\frac{1}{2} \rho \bar{u}^2 \right) \lambda \frac{L}{D_i} = q \lambda \frac{L}{D_i}$$

where

Δp = pressure loss in psi

$q = \frac{1}{2} \rho \bar{u}^2$ = dynamic pressure in psi

$\lambda = \lambda (re)$; Re = Reynolds number = $\frac{\bar{u} d}{\nu}$

A plot of λ versus Re is contained in Ref. 37

ν = kinematic viscosity

From Ref. 48, $\nu \cong 7.53 \times 10^{-6} \frac{ft^2}{sec}$

For an exit flow velocity of 1682 ft/sec through an 0.040" orifice, which are the conditions at which the water pumping system is required to operate, we can plot the pressure loss per foot of smooth straight tubing as a function of inside tube diameter. This is done in Fig. B-1.

Reference 48 in turn provides information that can be used to determine the length of smooth straight tubing which is equivalent to the various system components, such as valves, tees, and elbows. The following schematic diagram shows the various components in the water injection line between the accumulator and the water exit nozzle.

Table B-1 summarizes the expected pressure losses for each of the components shown. Thus at an accumulator pressure of 21,000 psi the exit pressure should be approximately 18,000 psi with a resulting velocity of approximately 1650 ft/second.

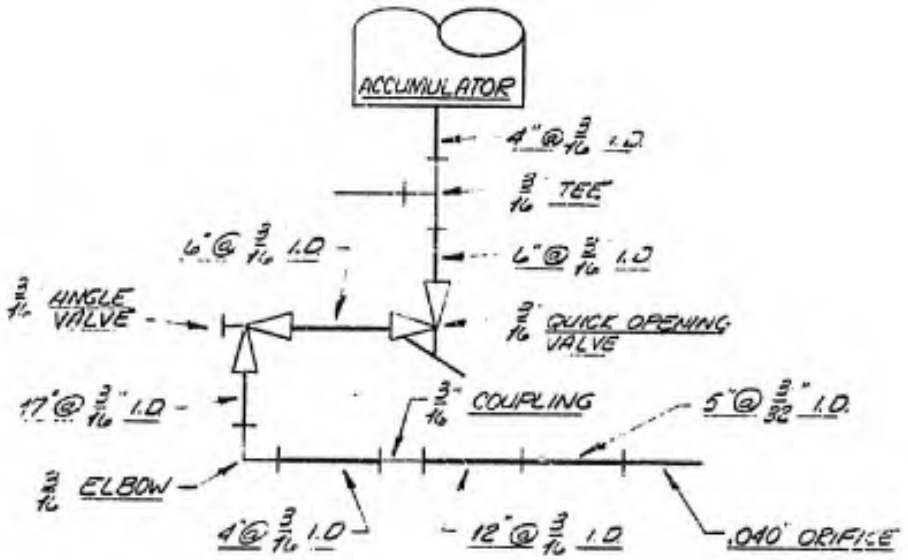

TABLE B-1. Pressure Losses in Pumping System

Item	Equivalent Length of Smooth Straight Tubing (inches)		Expected Pressure Loss (psi)
3/16" tubing	49	at 3/16"	196
3/32" tubing	5.58	at 3/32"	480
orifice	0.205	at 0.040"	1667
3/16" coupling	5	at 3/16"	20
3/16" elbow	10.7	at 3/16"	45
3/16" angle valve	37.5	at 3/16"	350
3/16" quick-opening valve	37.5	at 3/16"	450
3/16" tee	5	at 3/16"	20
Total			3226

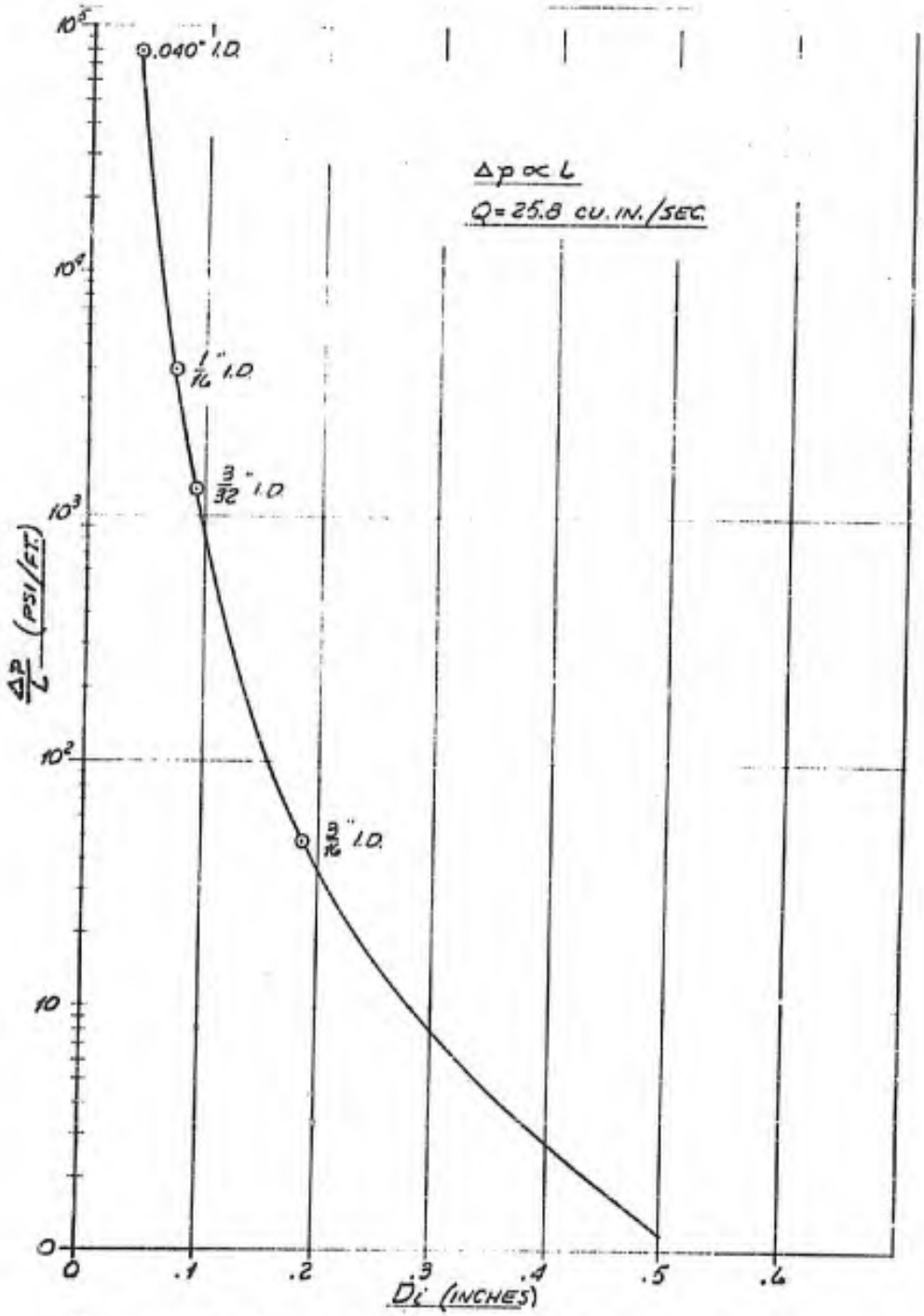

Figure B-1. Pressure loss per foot of smooth straight tubing.

MC-61-6-R1

CONFIDENTIAL

MITHRAS, Inc., 380 Putnam Ave., Cambridge 39, Mass.

RAIN EROSION SUPPRESSION AT SUPERSONIC SPEEDS (Unclassified Title) Interim Report. Contract Nonr 3684(00) xii and 98 pages. October 1962. CONFIDENTIAL

Laboratory tests of devices that can suppress rain erosion damage to supersonic aircraft and missiles by means of inducing drop breakup in separated flow regimes show that protection ranging from fair to excellent can be achieved. Equations are derived for both the drop breakup time and the drop breakup distance. The apparatus created for studying the erosion process and the water drop breakup process is described and the results of experiments conducted in a supersonic airstream are presented.

1. Radomes
2. Rain Erosion

I. MITHRAS Inc. MC-61-6-R1
II. Figler, Burton D.
III. Parkin, William J.
IV. Wilson, Jr. Joe C.

CONFIDENTIAL

MC-61-6-R1

CONFIDENTIAL

MITHRAS, Inc., 380 Putnam Ave., Cambridge 39, Mass.

RAIN EROSION SUPPRESSION AT SUPERSONIC SPEEDS (Unclassified Title) Interim Report. Contract Nonr 3684(00) xii and 98 pages. October 1962. CONFIDENTIAL

Laboratory tests of devices that can suppress rain erosion damage to supersonic aircraft and missiles by means of inducing drop breakup in separated flow regimes show that protection ranging from fair to excellent can be achieved. Equations are derived for both the drop breakup time and the drop breakup distance. The apparatus created for studying the erosion process and the water drop breakup process is described and the results of experiments conducted in a supersonic airstream are presented.

1. Radomes
2. Rain Erosion

I. MITHRAS Inc. MC-61-6-R1
II. Figler, Burton D.
III. Parkin, William J.
IV. Wilson, Jr. Joe C.

CONFIDENTIAL

MC-61-6-R1

CONFIDENTIAL

MITHRAS, Inc., 380 Putnam Ave., Cambridge 39, Mass.

RAIN EROSION SUPPRESSION AT SUPERSONIC SPEEDS (Unclassified Title) Interim Report. Contract Nonr 3684(00) xii and 98 pages. October 1962. CONFIDENTIAL

Laboratory tests of devices that can suppress rain erosion damage to supersonic aircraft and missiles by means of inducing drop breakup in separated flow regimes show that protection ranging from fair to excellent can be achieved. Equations are derived for both the drop breakup time and the drop breakup distance. The apparatus created for studying the erosion process and the water drop breakup process is described and the results of experiments conducted in a supersonic airstream are presented.

1. Radomes
2. Rain Erosion

I. MITHRAS Inc. MC-61-6-R1
II. Figler, Burton D
III. Parkin, William J.
IV. Wilson, Jr. Joe C.

CONFIDENTIAL

MC-61-6-R1

CONFIDENTIAL

MITHRAS, Inc., 380 Putnam Ave., Cambridge 39, Mass.

RAIN EROSION SUPPRESSION AT SUPERSONIC SPEEDS (Unclassified Title) Interim Report. Contract Nonr 3684(00) xii and 98 pages. October 1962. CONFIDENTIAL

Laboratory tests of devices that can suppress rain erosion damage to supersonic aircraft and missiles by means of inducing drop breakup in separated flow regimes show that protection ranging from fair to excellent can be achieved. Equations are derived for both the drop breakup time and the drop breakup distance. The apparatus created for studying the erosion process and the water drop breakup process is described and the results of experiments conducted in a supersonic airstream are presented.

1. Radomes
2. Rain Erosion

I. MITHRAS Inc. MC-61-6-R1
II. Figler, Burton D.
III. Parkin, William J.
IV. Wilson, Jr. Joe C.

CONFIDENTIAL

UNCLASSIFIED